

Angiotensin II attenuates myocardial interstitial acetylcholine release in response to vagal stimulation

Toru Kawada,¹ Toji Yamazaki,² Tsuyoshi Akiyama,² Meihua Li,^{1,3} Can Zheng,^{1,3} Toshiaki Shishido,¹ Hidezo Mori,² and Masaru Sugimachi¹

¹Department of Cardiovascular Dynamics, Advanced Medical Engineering Center and ²Department of Cardiac Physiology, National Cardiovascular Center Research Institute, Osaka; and ³Japan Association for the Advancement of Medical Equipment, Tokyo, Japan

Submitted 5 April 2007; accepted in final form 19 July 2007

Kawada T, Yamazaki T, Akiyama T, Li M, Zheng C, Shishido T, Mori H, Sugimachi M. Angiotensin II attenuates myocardial interstitial acetylcholine release in response to vagal stimulation. *Am J Physiol Heart Circ Physiol* 293: H2516–H2522, 2007. First published July 20, 2007; doi:10.1152/ajpheart.00424.2007.—Although ANG II exerts a variety of effects on the cardiovascular system, its effects on the peripheral parasympathetic neurotransmission have only been evaluated by changes in heart rate (an effect on the sinus node). To elucidate the effect of ANG II on the parasympathetic neurotransmission in the left ventricle, we measured myocardial interstitial ACh release in response to vagal stimulation (1 ms, 10 V, 20 Hz) using cardiac microdialysis in anesthetized cats. In a control group ($n = 6$), vagal stimulation increased the ACh level from 0.85 ± 0.03 to 10.7 ± 1.0 (SE) nM. Intravenous administration of ANG II at $10 \mu\text{g}\cdot\text{kg}^{-1}\cdot\text{h}^{-1}$ suppressed the stimulation-induced ACh release to 7.5 ± 0.6 nM ($P < 0.01$). In a group with pretreatment of intravenous ANG II receptor subtype 1 (AT₁ receptor) blocker losartan (10 mg/kg, $n = 6$), ANG II was unable to inhibit the stimulation-induced ACh release (8.6 ± 1.5 vs. 8.4 ± 1.7 nM). In contrast, in a group with local administration of losartan (10 mM, $n = 6$) through the dialysis probe, ANG II inhibited the stimulation-induced ACh release (8.0 ± 0.8 vs. 5.8 ± 1.0 nM, $P < 0.05$). In conclusion, intravenous ANG II significantly inhibited the parasympathetic neurotransmission through AT₁ receptors. The failure of local losartan administration to nullify the inhibitory effect of ANG II on the stimulation-induced ACh release indicates that the site of this inhibitory action is likely at parasympathetic ganglia rather than at postganglionic vagal nerve terminals.

cardiac microdialysis; cats; losartan

ANG II HAS a variety of effects on the cardiovascular system (22): it acts on the vascular beds to increase peripheral vascular resistance and also on the adrenal cortex to cause volume retention. These direct effects of ANG II contribute to the maintenance of arterial pressure (AP). Aside from these direct effects, ANG II has been shown to modulate the sympathetic nervous system both centrally (7, 9) and peripherally (10). With respect to the sympathetic regulation in the heart, however, exogenous ANG II does not facilitate stimulation- and ischemia-induced norepinephrine release in the porcine left ventricle (18). Compared with a number of reports on the sympathetic system, only a few reports are available as to the effects of ANG II on the parasympathetic system. In 1982, Potter (23) demonstrated that ANG II ($5\text{--}10 \mu\text{g}$ iv, body wt not

reported) inhibited bradycardia induced by vagal stimulation in dogs. In that study, administration of ACh reduced the heart rate to an identical degree in the presence or absence of ANG II, suggesting that the inhibition of bradycardia by ANG II was attributable to the inhibition of the ACh release from the vagal nerve terminals. In contrast, Andrews et al. (3) reported that ANG II (500 ng/kg iv) did not inhibit bradycardia induced by vagal stimulation in ferrets. In a rat heart failure model, ANG II receptor subtype 1 (AT₁ receptor) antagonist losartan enhanced the bradycardic response to vagal stimulation (5). In pithed rats, an angiotensin-converting enzyme (ACE) inhibitor captopril also enhanced the bradycardic response to vagal stimulation (25, 26). In all of these studies, changes in the heart rate were used as a functional measurement of peripheral vagal function because of the difficulty in measuring the ACh release in the in vivo heart. Accordingly, whether ANG II affects the vagal control over the ventricle remains unknown. The aim of the present study was to examine the effect of ANG II on the vagal stimulation-induced ACh release in the left ventricular myocardium by measuring the interstitial ACh levels directly using a cardiac microdialysis technique (1, 13–15). We also explored the possible sites of action for the effect of ANG II on the stimulation-induced ACh release by administering losartan systemically from the femoral vein or locally through the dialysis fiber. Because ACh has a protective effect on the ischemic myocardium (12, 24, 29), elucidating the effect of ANG II on the ACh release in the ventricle would be helpful to understand the mechanism of ACE inhibitor or AT₁ receptor antagonist for the treatment of heart diseases (16, 17).

MATERIALS AND METHODS

Surgical Preparation

Animal care was provided in strict accordance with the *Guiding Principles for the Care and Use of Animals in the Field of Physiological Sciences* approved by the Physiological Society of Japan. All protocols were approved by the Animal Subject Committee of the National Cardiovascular Center. Twenty eight adult cats weighing from 1.9 to 4.9 kg were anesthetized using an intraperitoneal injection of pentobarbital sodium ($30\text{--}35 \text{ mg/kg}$) and were then ventilated mechanically with room air mixed with oxygen. The depth of anesthesia was maintained by a continuous intravenous infusion of pentobarbital sodium ($1\text{--}2 \text{ mg}\cdot\text{kg}^{-1}\cdot\text{h}^{-1}$) through a catheter inserted in the right femoral vein. Systemic AP was monitored by a catheter inserted in the right femoral artery. Heart rate was determined from an

Address for reprint requests and other correspondence: T. Kawada, Dept. of Cardiovascular Dynamics, National Cardiovascular Center Research Institute, 5-7-1 Fujishirodai, Suita, Osaka 565-8565, Japan (e-mail: torukawa@res.nccv.go.jp).

The costs of publication of this article were defrayed in part by the payment of page charges. The article must therefore be hereby marked "advertisement" in accordance with 18 U.S.C. Section 1734 solely to indicate this fact.

electrocardiogram using a cardi tachometer. Esophageal temperature of the animal, measured using a thermometer (CTM-303; TERUMO), was maintained at $\sim 37^{\circ}\text{C}$ using a heating pad and a lamp. Both vagal nerves were exposed and sectioned bilaterally through a midline cervical incision. With the animal in the lateral position, we resected the left fifth and sixth ribs to approach the heart. After the incision of the pericardium, the heart was suspended in a pericardial cradle. Stainless steel wires were attached to the apex and the posterior wall of the left ventricle to pace the heart. Using a fine guiding needle, we implanted a dialysis probe transversely through the anterolateral free wall of the left ventricle. Next, we attached a pair of bipolar platinum electrodes to the cardiac end of each sectioned vagal nerve. The nerves and electrodes were covered in warmed mineral oil for insulation. We gave heparin sodium (100 U/kg) intravenously to prevent blood coagulation. At the end of the experiment, postmortem examination confirmed that the semipermeable membrane of the dialysis probe had been implanted in the left ventricular myocardium.

Dialysis Technique

The materials and properties of the dialysis probe have been described previously (1). Briefly, we designed a transverse dialysis probe in which a dialysis fiber of semipermeable membrane (13 mm length, 310 μm outer diameter, 200 μm inner diameter; PAN-1200, 50,000 mol wt cutoff; Asahi Chemical) was attached at both ends to

polyethylene tubes (25 cm length, 500 μm outer diameter, 200 μm inner diameter). The dialysis probe was perfused at a rate of 2 $\mu\text{l}/\text{min}$ with Ringer solution containing the cholinesterase inhibitor physostigmine (100 μM). Experimental protocols were started 2 h after implanting the dialysis probe when the ACh concentration in the dialysate reached a steady state. ACh concentrations in the dialysate were measured by an HPLC system with electrochemical detection (Eicom, Kyoto, Japan).

Figure 1 schematizes the three original protocols and two supplemental protocols utilized in the present study. The hatched rectangle indicates the baseline sampling, whereas the solid rectangles indicate the sampling during the 10-min vagal stimulation period (1 ms, 10 V, 20 Hz) in each protocol. The stimulus was set supramaximal to most easily delineate the possible effect of ANG II on myocardial interstitial ACh release. In all of the vagal stimulation periods, we paced the heart at 200 beats/min to avoid the difference in heart rate affecting the vagal stimulation-induced ACh release (14). For baseline sampling periods, we paced the heart at 200 beats/min when spontaneous heart rate was < 200 beats/min.

Protocol 1 ($n = 6$). We examined the effects of intravenous administration of ANG II on vagal stimulation-induced myocardial ACh release. We collected a dialysate sample under baseline conditions. We then stimulated the vagal nerve and paced the heart for 10 min and collected a dialysate sample during the stimulation period

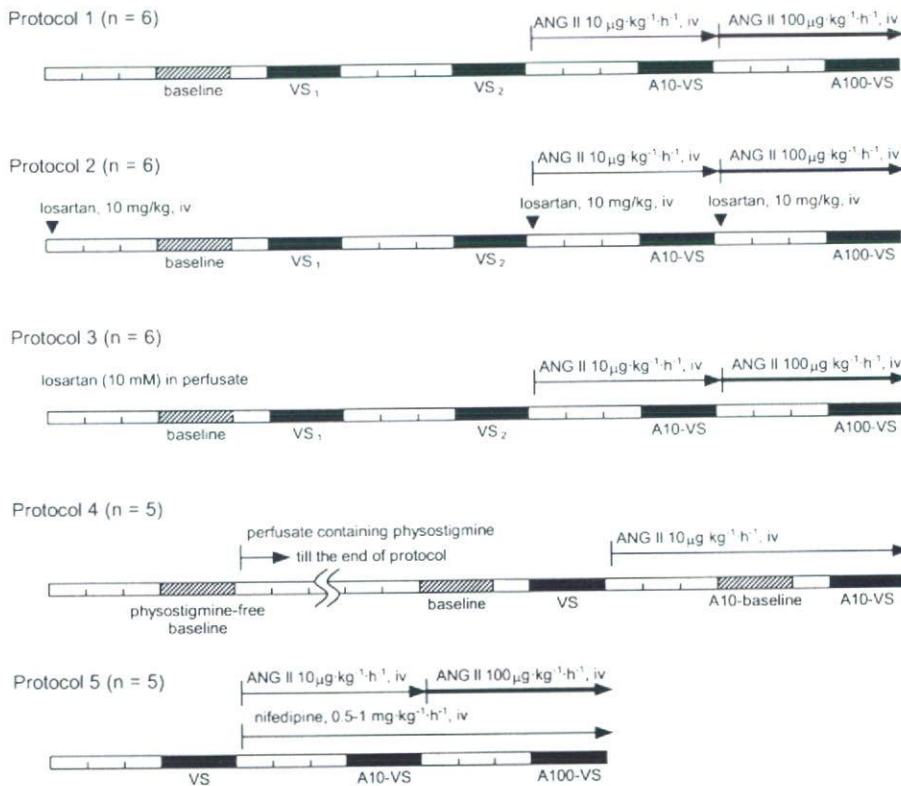


Fig. 1. Schematic representation of the protocols used in the present study. After implantation of the dialysis probe (2 h), we obtained a baseline dialysate sample (hatched rectangles) for 10 min. Thereafter, we obtained 4 dialysate samples during vagal stimulation with fixed-rate pacing for 10 min (filled rectangles) at intervening intervals of 15 min. In *protocols 1* through *3*, after obtaining 2 control trials (VS_1 and VS_2), we initiated intravenous administration of ANG II at $10 \mu\text{g}\cdot\text{kg}^{-1}\cdot\text{h}^{-1}$ and waited for 15 min to obtain a dialysate sample during vagal stimulation with fixed-rate pacing (A10-VS). We then increased the dose of ANG II to $100 \mu\text{g}\cdot\text{kg}^{-1}\cdot\text{h}^{-1}$ and waited for an additional 15 min before obtaining a dialysate sample during vagal stimulation with fixed-rate pacing (A100-VS). In *protocol 2*, the ANG II receptor subtype 1 blocker losartan was administered by bolus injection (10 mg/kg) before obtaining a baseline dialysate sample and also immediately before the beginning of each dose of ANG II administration (\blacktriangledown). In *protocol 3*, we administered losartan (10 mM) through the dialysis probe throughout the protocol. In *protocol 4*, we first collected a dialysate sample using perfusate free of physostigmine. We then replaced the perfusate with Ringer solution containing physostigmine and collected dialysate samples of baseline and vagal stimulation (VS). Approximately 15 min after the onset of iv ANG II administration at $10 \mu\text{g}\cdot\text{kg}^{-1}\cdot\text{h}^{-1}$, we collected dialysate samples of baseline (A10-baseline) and vagal stimulation (A10-VS). In *protocol 5*, we collected dialysate samples during a control vagal stimulation (VS) and during the 2 doses of iv ANG II administration (A10-VS and A100-VS). The pressor effect of ANG II was counteracted by simultaneous iv infusion of the L-type Ca^{2+} channel blocker nifedipine.

(VS₁). After an intervening interval of 15 min, we repeated the 10-min vagal stimulation with fixed-rate pacing and collected another dialysate sample (VS₂). After performing these two control trials, we began intravenous administration of ANG II at 10 $\mu\text{g}\cdot\text{kg}^{-1}\cdot\text{h}^{-1}$. Approximately 15 min after the onset of the ANG II administration, we collected a dialysate sample (A10-VS) during 10-min vagal stimulation with fixed-rate pacing. We then increased the dose of ANG II at 100 $\mu\text{g}\cdot\text{kg}^{-1}\cdot\text{h}^{-1}$. Approximately 15 min after the onset of the higher-dose ANG II administration, we collected a final dialysate sample (A100-VS) during 10-min vagal stimulation with fixed-rate pacing.

Protocol 2 ($n = 6$). We examined whether the intravenous AT₁ receptor antagonist losartan would block the effects of ANG II on the vagal stimulation-induced myocardial ACh release. We infused losartan potassium intravenously at 10 mg/kg and waited for ~15 min. We then collected baseline, VS₁, and VS₂ samples with an intervening interval of 15 min, as described in *protocol 1*. Next, after an additional bolus injection of losartan potassium at 10 mg/kg, we began intravenous infusion of ANG II at 10 $\mu\text{g}\cdot\text{kg}^{-1}\cdot\text{h}^{-1}$. After ~15 min, we obtained a dialysate sample of A10-VS. Finally, after another bolus injection of losartan potassium at 10 mg/kg, we began intravenous infusion of ANG II at 100 $\mu\text{g}\cdot\text{kg}^{-1}\cdot\text{h}^{-1}$. After an additional 15 min, we obtained a dialysate sample of A100-VS.

Protocol 3 ($n = 6$). We examined whether local administration of losartan would block the effects of ANG II on the vagal stimulation-induced myocardial ACh release. We perfused the dialysis probe with Ringer solution containing 10 mM of losartan potassium. Taking into account the distribution across the semipermeable membrane, we administered losartan at a concentration >400 times higher than that for intravenous administration in *protocol 2*. Because local administrations of larger molecules such as ω -conotoxin GVIA (molecular weight 3037) and ω -conotoxin MVIIC (mol wt 2,749) were able to suppress vagal stimulation-induced ACh release in our previous study (15), it would be reasonable to assume that losartan potassium (mol wt 461) should have spread in the vicinity of the dialysis fiber, from which the dialysate was collected. Using the same procedures as described in *protocol 1*, we obtained dialysate samples for baseline, VS₁, VS₂, A10-VS, and A100-VS. A previous study indicated that ACh measured by cardiac microdialysis in the left ventricle mainly reflected ACh released from the postganglionic nerve terminals and not from the parasympathetic ganglia (1 and see DISCUSSION for details).

Protocol 4 ($n = 5$). To examine the effects of ANG II on the baseline ACh level, we performed an additional protocol where the baseline ACh level was measured during intravenous infusion of

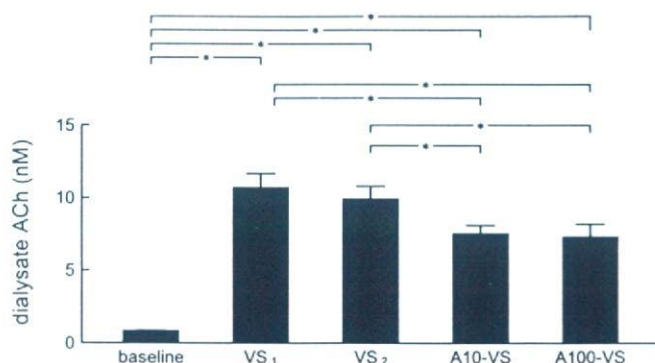


Fig. 2. Changes in dialysate ACh concentrations obtained from *protocol 1*. Vagal stimulation significantly increased the ACh levels. There was no significant difference in the ACh level between the 2 control trials (VS₁ and VS₂). The ACh level was significantly lower in A10-VS and A100-VS compared with that measured in VS₁ and VS₂. There was no significant difference in the ACh level between A10-VS and A100-VS. Values are presented as mean and SE. * $P < 0.01$ by Tukey's test.

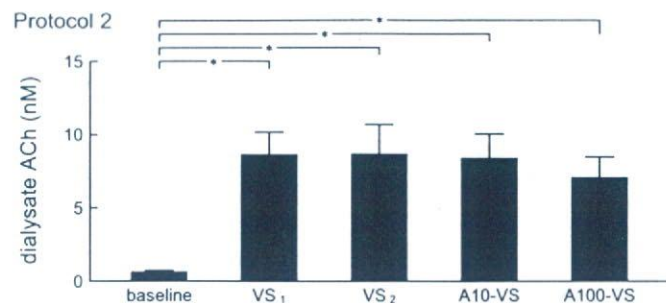


Fig. 3. Changes in dialysate ACh concentrations obtained from *protocol 2*. Vagal stimulation significantly increased the ACh levels. There was no significant difference in the ACh level among the 4 dialysate samples during vagal stimulation (VS₁, VS₂, A10-VS, and A100-VS). Values are presented as means and SE. * $P < 0.01$ by Tukey's test.

ANG II at 10 $\mu\text{g}\cdot\text{kg}^{-1}\cdot\text{h}^{-1}$ (A10-baseline). In this protocol, we also obtained a dialysate sample using the perfusate without the cholinesterase inhibitor physostigmine before the usual dialysate sampling using the perfusate containing physostigmine.

Protocol 5 ($n = 5$). To avoid the pressor effect of ANG II, we administered an L-type Ca²⁺ channel blocker nifedipine (0.5–2.0 mg·kg⁻¹·h⁻¹) simultaneously with ANG II and obtained dialysate samples for VS, A10-VS, and A100-VS. In a previous study, intravenous administration of an L-type Ca²⁺ channel blocker alone did not affect the vagal stimulation-induced myocardial ACh release significantly (15).

Statistical Analysis

All data are presented as mean \pm SE values. In *protocols 1* through *3*, myocardial interstitial ACh levels were compared among baseline, VS₁, VS₂, A10-VS, and A100-VS samples using a repeated-measures ANOVA (8). When there was a significant difference, Tukey's test for all-pairwise comparisons was applied to identify the differences between any two of the samples. Differences were considered significant at $P < 0.05$. The mean AP value in the last 1 min of the 10-min vagal stimulation period was treated as the AP value during vagal stimulation. The AP data were compared using a repeated-measures ANOVA among baseline, during the two control stimulations (VS₁ and VS₂), and before and during vagal stimulation under the two different doses of intravenous ANG II administrations. When there was a significant difference, Dunnett's test for comparison against a single control was applied to identify differences from the baseline value. Differences were considered significant at $P < 0.05$. In

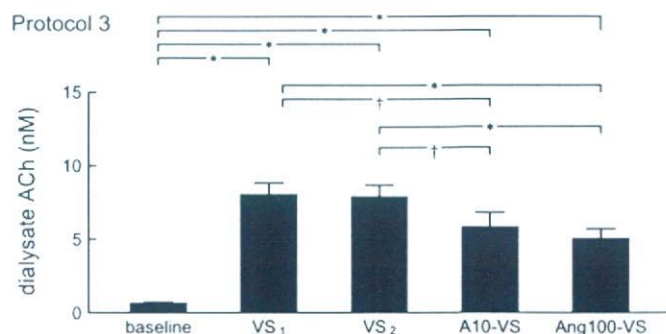


Fig. 4. Changes in dialysate ACh concentrations obtained from *protocol 3*. Vagal stimulation significantly increased the ACh levels. There was no significant difference in the ACh level between the 2 control trials (VS₁ and VS₂). The ACh level was significantly lower in A10-VS and A100-VS compared with that measured in VS₁ and VS₂. There was no significant difference in the ACh level between A10-VS and A100-VS. Values are presented as means and SE. † $P < 0.05$ and * $P < 0.01$ by Tukey's test.

Table 1. Mean arterial pressure values before vagal stimulation and during the last 1 min of stimulation

	Baseline	VS ₁	VS ₂	A10	A10-VS	A100	A100-VS
Protocol 1	102 ± 11	93 ± 17	91 ± 17	132 ± 9†	105 ± 19	129 ± 13†	105 ± 21
Protocol 2	102 ± 17	71 ± 16*	69 ± 16*	80 ± 15	68 ± 17*	86 ± 19	72 ± 18*
Protocol 3	102 ± 13	100 ± 17	92 ± 17	139 ± 11*	120 ± 19	147 ± 11*	122 ± 21

Data are means ± SE obtained from baseline, two control trials (VS₁ and VS₂), before (A10) and during (A10-VS) vagal stimulation under iv administration of ANG II at 10 $\mu\text{g}\cdot\text{kg}^{-1}\cdot\text{h}^{-1}$, and before (A100) and during (A100-VS) vagal stimulation under iv administration of ANG II at 100 $\mu\text{g}\cdot\text{kg}^{-1}\cdot\text{h}^{-1}$. The heart was paced at 200 beats/min whenever vagal stimulation was applied. † $P < 0.05$ and * $P < 0.01$ from the respective baseline values by Dunnett's test.

protocol 4, the baseline ACh levels were compared before and during the ANG II administration using a paired *t*-test. The ACh levels during vagal stimulation were also compared before and during ANG II administration using a paired *t*-test. In protocol 5, the ACh levels and the mean AP values were compared among VS, A10-VS, and A100-VS using a repeated-measures ANOVA followed by Tukey's test.

RESULTS

In protocol 1, vagal stimulation significantly increased myocardial interstitial ACh levels (Fig. 2). There was no significant difference between two control trials with an intervening interval of 15 min [VS₁: 10.7 ± 1.0 (SE) nM and VS₂: 9.9 ± 0.9 (SE) nM]. Intravenous administration of ANG II at 10 $\mu\text{g}\cdot\text{kg}^{-1}\cdot\text{h}^{-1}$ significantly attenuated the vagal stimulation-induced ACh release (A10-VS: 7.5 ± 0.6 nM) to ~71% of VS₁. Although the intravenous administration of ANG II at 100 $\mu\text{g}\cdot\text{kg}^{-1}\cdot\text{h}^{-1}$ also significantly attenuated the vagal stimulation-induced ACh release (A100-VS: 7.3 ± 0.9 nM) to ~68% of VS₁, the ACh levels were not different from those of A10-VS.

In protocol 2, vagal stimulation significantly increased myocardial interstitial ACh levels under control stimulations (VS₁: 8.6 ± 1.5 nM and VS₂: 8.7 ± 2.0 nM; Fig. 3). With a pretreatment of intravenous losartan, intravenous ANG II was unable to suppress the vagal stimulation-induced ACh release (A10-VS: 8.4 ± 1.7 nM and A100-VS: 7.1 ± 1.4 nM). Although the mean level of ACh tended to be lower in A100-VS compared with VS₁ or VS₂, the differences were not statistically significant.

In protocol 3, vagal stimulation significantly increased myocardial interstitial ACh levels under control stimulations (VS₁: 8.0 ± 0.8 nM and VS₂: 7.9 ± 0.8 nM; Fig. 4). Intravenous

ANG II at either 10 $\mu\text{g}\cdot\text{kg}^{-1}\cdot\text{h}^{-1}$ or 100 $\mu\text{g}\cdot\text{kg}^{-1}\cdot\text{h}^{-1}$ significantly suppressed the vagal stimulation-induced ACh release to ~72% (A10-VS: 5.8 ± 1.0 nM) and 62% (A100-VS: 5.0 ± 0.7 nM of that seen in VS₁), respectively.

In protocol 1, the AP values before the vagal stimulation during the intravenous ANG II administrations (A10 and A100) were significantly higher than the baseline AP value (Table 1). The AP values during vagal stimulation (VS₁, VS₂, A10-VS, and A100-VS) were not different from the baseline AP value. In protocol 2, the AP value before the first administration of losartan was 126 ± 14 mmHg. The AP values before the vagal stimulation during the intravenous ANG II administrations (A10 and A100) were not significantly different from the baseline AP value. The AP values during vagal stimulation (VS₁, VS₂, A10-VS, and A100-VS) were significantly lower than the baseline AP value. In protocol 3, the AP values before vagal stimulation during the intravenous ANG II administrations (A10 and A100) were significantly higher than the baseline AP value. The AP values during vagal stimulation (VS₁, VS₂, A10-VS, and A100-VS) did not differ statistically from the baseline AP value.

Figure 5 illustrates typical chromatograms obtained from one animal in protocol 4. The baseline ACh level was below the limit of determination (0.5 nM) when the perfusate did not contain physostigmine (physostigmine-free baseline). The baseline ACh level was above the limit of determination. As shown in Table 2, vagal stimulation significantly increased the ACh level (VS). The intravenous administration of ANG II did not affect the baseline ACh level (A10-baseline) but significantly attenuated the ACh level during vagal stimulation (A10-VS).

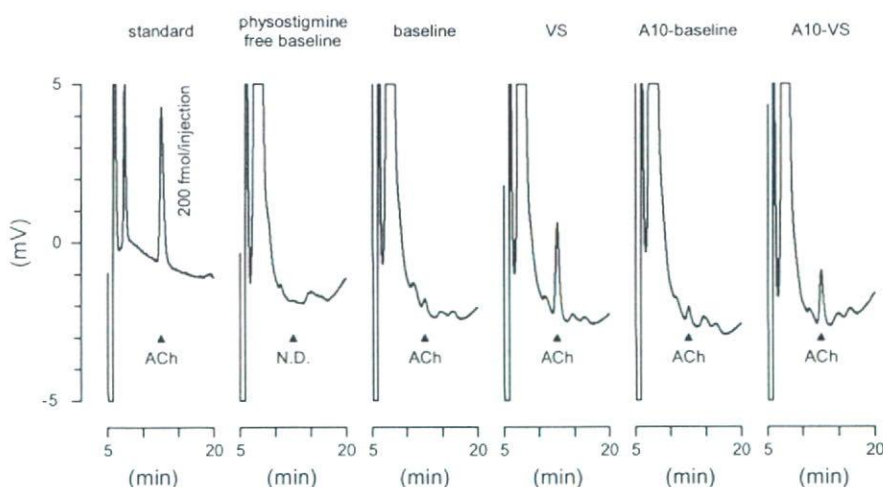


Fig. 5. Typical chromatograms for the ACh measurements obtained from protocol 4. ACh was less than the limit of determination when perfusate did not contain physostigmine (physostigmine-free baseline). The baseline ACh level was above the limit of determination when perfusate contained 100 μM physostigmine. (This perfusate was usually used for the ACh measurements.) Vagal stimulation increased the ACh level (VS). The administration of ANG II at 10 $\mu\text{g}\cdot\text{kg}^{-1}\cdot\text{h}^{-1}$ did not affect baseline ACh level (A10-baseline) but significantly attenuated the vagal stimulation-induced ACh release (A10-VS). See Table 2 for pooled data of ACh levels. ND, not detected.

Table 2. Mean arterial pressure values and ACh concentrations obtained in protocol 4

	Physostigmine-free Baseline	Baseline	VS	A10-Baseline	A10-VS
ACh, nM	Not detected	1.6 ± 0.4	10.6 ± 2.4	1.7 ± 0.5	7.8 ± 2.1*
Mean arterial pressure, mmHg	111 ± 11	109 ± 12	103 ± 6	148 ± 3*	118 ± 6

Data are means ± SE obtained from physostigmine-free baseline, baseline, control vagal stimulation (VS), and baseline (A10-baseline) and vagal stimulation (A10-VS) under iv administration of ANG II at 10 $\mu\text{g}\cdot\text{kg}^{-1}\cdot\text{h}^{-1}$. There was no significant difference in the ACh level between baseline and A10-baseline by a paired-*t*-test. The ACh level was significantly lower in A10-VS than in VS by a paired-*t*-test. Mean arterial pressure was significantly higher in A10-baseline compared with the physostigmine-free baseline value by Dunnett's test. **P* < 0.01.

In protocol 5, the pressor effect of ANG II was counteracted by the simultaneous intravenous infusion of nifedipine (Table 3). Under this condition, the intravenous administration of ANG II significantly attenuated the stimulation-induced ACh level to ~83% (A10-VS) and 72% (A100-VS) of that seen in VS.

DISCUSSION

The present study demonstrated that intravenous ANG II significantly inhibited the vagal stimulation-induced myocardial interstitial ACh release in the left ventricle in anesthetized cats. Intravenous administration of losartan abolished the inhibitory effect of ANG II on the stimulation-induced ACh release, suggesting that the inhibitory action of ANG II was mediated by AT₁ receptors.

Inhibitory Effect of ANG II on Myocardial Interstitial ACh Release

Only a few reports have focused on the modulatory effects of ANG II on the parasympathetic nervous system (3, 5, 25, 26), all of which have used the heart rate reduction in response to vagal stimulation as a functional measurement to assess the peripheral vagal function. Although ANG II has been shown to inhibit the ACh release in the rat entorhinal cortex *in vitro* (4), the direct evidence for the inhibitory effect of ANG II on the ACh release in the peripheral vagal neurotransmission *in vivo* has been lacking. The present study demonstrated that intravenous ANG II inhibited the vagal nerve stimulation-induced ACh release in the left ventricle *in vivo* (Fig. 2). As for the sympathetic system in the heart, Lameris et al. (18) have previously demonstrated that ANG II does not affect the sympathetic nerve stimulation-induced norepinephrine release. The in-

Table 3. Mean arterial pressure values and ACh concentrations obtained in protocol 5

	VS	A10-VS	A100-VS
ACh, nM	12.7 ± 1.1	10.6 ± 1.1†	9.2 ± 1.5*
Mean arterial pressure, mmHg	83.4 ± 12.2	68.4 ± 6.3	70.4 ± 9.5

Data are means ± SE from a control vagal stimulation trial (VS), during vagal stimulation under iv administration of ANG II at 10 $\mu\text{g}\cdot\text{kg}^{-1}\cdot\text{h}^{-1}$ (A10-VS) and during vagal stimulation under iv administration of ANG II at 100 $\mu\text{g}\cdot\text{kg}^{-1}\cdot\text{h}^{-1}$ (A100-VS). The heart was paced at 200 beats/min during vagal stimulation. In this protocol, the pressor effect of ANG II was counteracted by simultaneous iv administration of the L-type Ca²⁺ channel blocker nifedipine (0.5–2 $\text{mg}\cdot\text{kg}^{-1}\cdot\text{h}^{-1}$). †*P* < 0.05 and **P* < 0.01 from the VS group by Tukey's test. There was no significant difference between A10-VS and A100-VS in the ACh level. There were no significant differences in mean arterial pressure among the three trials.

significant effect of ANG II on the sympathetic neurotransmission and the inhibitory effect of ANG II on the parasympathetic neurotransmission may provide the basis for a study by Takata et al. (26) in which ACE inhibitor enhanced cardiac vagal but not sympathetic neurotransmission.

An increased activity of the renin-angiotensin system is common in chronic heart failure and has been considered to be a stimulus for aggravation of the disease. Inhibition of the renin-angiotensin system by ACE inhibitors or by AT₁ receptor blockers can prevent the ventricular remodeling and improve the survival rate (16, 17), suggesting that ANG II is indeed involved in the aggravation of heart failure. ACh, on the other hand, can exert a cardioprotective effect against myocardial ischemia in several experimental settings (12, 24, 29). If ANG II inhibits the peripheral vagal neurotransmission, blockade of ANG II would increase the vagal effect on the heart. Actually, Du et al. (5) demonstrated that losartan enhanced bradycardia induced by vagal stimulation in rats with chronic myocardial infarction. In that study, however, the ventricular effect of vagal stimulation was not assessed. The results of the present study indicate that ANG II inhibited the vagal neurotransmission in the ventricle. Blockade of ANG II is therefore expected to increase the vagal effect on the ventricular myocardium when the vagal outflow from the central nervous system is unchanged. Although no literatures appear to be available as to the chronic effect of ACh on the prognosis of heart failure, electrical vagal stimulation was able to improve the survival rate of chronic heart failure in rats (19). In that study, the magnitude of the vagal stimulation was such that the heart rate decreased only by 20–30 beats/min in rats, suggesting that a modest increase in vagal tone would be sufficient to produce a cardioprotective effect. It is plausible that blockade of ANG II yields beneficial effects on chronic heart failure not only by antagonizing the sympathetic effects but also by enhancing the vagal effects on the ventricle.

Vagal stimulation was able to reduce the left ventricular contractility as assessed by end-systolic elastance only when sympathetic stimulation coexisted (20), suggesting that the effect of vagal stimulation on ventricular contractility would be secondary to sympathoinhibition. Accordingly, contribution of the inhibitory effect of ANG II on the stimulation-induced ACh release to the physiological regulation of ventricular contractility might be marginal. We think that the finding is important as a peripheral mechanism of vagal withdrawal in heart diseases accompanying the activation of the renin-angiotensin system.

Possible Site of the Inhibitory Action of ANG II on ACh Release

In *protocol 3*, we examined whether local administration of losartan was able to nullify the inhibitory effect of ANG II on the vagal stimulation-induced ACh release. The utility of local administration of pharmacological agents through the dialysis fiber has been confirmed previously. As an example, local administration the Na⁺ channel inhibitor tetrodotoxin through the dialysis fiber completely blocked the nerve stimulation-induced ACh release (14). With respect to the source for ACh, intravenous administration of the nicotinic antagonist hexamethonium bromide completely blocked the stimulation-induced ACh release, whereas local administration of hexamethonium bromide did not, suggesting the lack of parasympathetic ganglia in the vicinity of dialysis fiber (1). In support of our interpretation, a neuroanatomic finding indicates that three ganglia, away from the left anterior free wall targeted by the dialysis probe, provide the major source of left ventricular postganglionic innervation in cats (11). Therefore, the myocardial interstitial ACh measured by cardiac microdialysis in the left ventricle mainly reflects the ACh release from the postganglionic vagal nerve terminals. The results of *protocol 3* indicate that losartan spread around the postganglionic vagal nerve terminals failed to abolish the inhibitory effect of ANG II on the stimulation-induced ACh release. Because intravenous administration of losartan was able to abolish the inhibitory effect of ANG II on the stimulation-induced ACh release (*protocol 2*), the site of this inhibitory action is likely at parasympathetic ganglia rather than at postganglionic vagal nerve terminals. The fact that AT₁ receptors are rich in parasympathetic ganglia (2) would support our interpretation.

ANG II has a direct vasoconstrictive effect on the coronary artery (30). At the same time, however, the intravenous administration of ANG II tended to increase mean AP during vagal stimulation by ~15 mmHg in *protocol 1* (Table 1). Although it was statistically insignificant, if this increase in mean AP increased cardiac oxygen demand, the coronary blood flow might have been increased (27), resulting in an increased rate of washout in the myocardial tissue. The possibility cannot be ruled out that such a washout mechanism contributed to the reduction of stimulation-induced ACh release during ANG II administration. However, the baseline ACh level was not decreased by ANG II in *protocol 4*, suggesting that the washout rate did not increase significantly. In addition, even when the pressor effect of ANG II was counteracted by nifedipine, ANG II was still able to inhibit the vagal stimulation-induced ACh release in *protocol 5*. Therefore, we think that the change in washout rate was not a principal mechanism for the reduction of stimulation-induced ACh release by ANG II.

The mechanisms for the baseline ACh release under the vagotomized condition were not identified in the present study. In the motor nerve terminals, a so-called nonquantal release of ACh is documented, which is independent of nerve activity (6). Incorporation of the vesicular transport system in the membrane of the nerve terminals during an exocytosis process is considered to be responsible for the mechanism of nonquantal ACh release. A similar mechanism might contribute to the baseline ACh release in the vagal nerve terminals.

Several limitations need to be addressed. First, the dose of ANG II might have increased the plasma ANG II concentration

beyond the physiological range. In this regard, the observed effect might be rather pharmacological or pathological than physiological. Nevertheless, because there are local synthesis and degradation of ANG II in the heart (21, 28), the inhibition of ACh release by ANG II could operate locally in the heart. Second, whether ANG II inhibited the ACh release from the preganglionic nerve terminals or it suppressed the excitability of the postganglionic nerve fibers to ACh was not identified in the present study. Third, the involvement of ANG II receptor subtype 2 (AT₂ receptor) in the modulation of peripheral parasympathetic neurotransmission was not examined in the present study because intravenous losartan was able to abolish the inhibitory effect of ANG II on the stimulation-induced ACh release. However, if coactivation of AT₁ and AT₂ receptors is required for the inhibitory effect of ANG II, blockade of AT₂ receptors would also abolish the inhibitory effect. Fourth, we tested just one level of vagal stimulation. Whether the effect of ANG II on the stimulation-induced ACh release depends on the vagal stimulation intensity remains to be resolved.

In conclusion, intravenous ANG II reduced the vagal nerve stimulation-induced ACh release in the left ventricle. Intravenous losartan abolished the inhibitory effect of ANG II on the stimulation-induced ACh release, suggesting that this inhibition was mediated by AT₁ receptors. Because local administration of losartan via dialysis fiber was unable to nullify the inhibitory effect of ANG II on the stimulation-induced ACh release, the site of this inhibitory action is likely parasympathetic ganglia. The present results imply that the beneficial effects of ACE inhibitors and AT₁ receptor antagonists in the treatment of heart diseases may include not only the suppression of sympathetic activity but also the enhancement of vagal activity to the ventricle.

GRANTS

This study was supported by a Health and Labour Sciences Research Grant for Research on Advanced Medical Technology, a Health and Labour Sciences Research Grant for Research on Medical Devices for Analyzing, Supporting, and Substituting the Function of Human Body, and Health and Labour Sciences Research Grant H18-iryō-Ippan-023 from the Ministry of Health, Labour, and Welfare of Japan.

REFERENCES

1. Akiyama T, Yamazaki T, Ninomiya I. In vivo detection of endogenous acetylcholine release in cat ventricles. *Am J Physiol Heart Circ Physiol* 266: H854–H860, 1994.
2. Allen AM, Zhuo J, Mendelsohn FA. Localization and function of angiotensin AT₁ receptors. *Am J Hypertens* 13: 31S–38S, 2000.
3. Andrews PL, Dutia MB, Harris PJ. Angiotensin II does not inhibit vagally-induced bradycardia or gastric contractions in the anaesthetized ferret. *Br J Pharmacol* 82: 833–837, 1984.
4. Barnes JM, Barnes NM, Costall B, Horovitz ZP, Naylor RJ. Angiotensin II inhibits the release of [³H]acetylcholine from rat entorhinal cortex in vitro. *Brain Res* 491: 136–143, 1989.
5. Du XJ, Cox HS, Dart AM, Esler MD. Depression of efferent parasympathetic control of heart rate in rats with myocardial infarction: effect of losartan. *J Cardiovasc Pharmacol* 31: 937–944, 1998.
6. Edwards C, Doležal V, Tuček S, Zemková H, Vyskočil F. Is an acetylcholine transport system responsible for nonquantal release of acetylcholine at the rodent myoneural junction? *Proc Natl Acad Sci USA* 82: 3354–3358, 1985.
7. Gao L, Wang W, Li Y, Schultz HD, Liu D, Cornish KG, Zucker IH. Sympathoexcitation by central ANG II: roles for AT₁ receptor upregulation and NAD(P)H oxidase in RVLM. *Am J Physiol Heart Circ Physiol* 288: H2271–H2279, 2005.
8. Glantz SA. *Primer of Biostatistics* (5th ed.). New York: McGraw-Hill, 2002.

9. Hirooka Y, Head GA, Potts PD, Godwin SJ, Bendle RD, Dampney RA. Medullary neurons activated by angiotensin II in the conscious rabbit. *Hypertension* 27: 287–296, 1996.
10. Hughes J, Roth RH. Evidence that angiotensin enhances transmitter release during sympathetic nerve stimulation. *Br J Pharmacol* 41: 239–255, 1971.
11. Johnson TA, Gray AL, Lauenstein JM, Newton SS, Massari VJ. Parasympathetic control of the heart. I. An interventriculo-septal ganglion is the major source of the vagal intracardiac innervation of the ventricles. *J Appl Physiol* 96: 2265–2272, 2004.
12. Kakinuma Y, Ando M, Kuwabara M, Katara RG, Okudela K, Kobayashi M, Sato T. Acetylcholine from vagal stimulation protects cardiomyocytes against ischemia and hypoxia involving additive non-hypoxic induction of HIF-1 α . *FEBS Lett* 579: 2111–2118, 2005.
13. Kawada T, Yamazaki T, Akiyama T, Sato T, Shishido T, Inagaki M, Takaki H, Sugimachi M, Sunagawa K. Differential acetylcholine release mechanisms in the ischemic and non-ischemic myocardium. *J Mol Cell Cardiol* 32: 405–414, 2000.
14. Kawada T, Yamazaki T, Akiyama T, Shishido T, Inagaki M, Uemura K, Miyamoto T, Sugimachi M, Takaki H, Sunagawa K. In vivo assessment of acetylcholine-releasing function at cardiac vagal nerve terminals. *Am J Physiol Heart Circ Physiol* 281: H139–H145, 2001.
15. Kawada T, Yamazaki T, Akiyama T, Uemura K, Kamiya A, Shishido T, Mori H, Sugimachi M. Effects of Ca²⁺ channel antagonists on nerve stimulation-induced and ischemia-induced myocardial interstitial acetylcholine release in cats. *Am J Physiol Heart Circ Physiol* 291: H2187–H2191, 2006.
16. Konstam MA, Neaton JD, Poole-Wilson PA, Pitt B, Segal R, Sharma D, Dasbach EJ, Carides GW, Dickstein K, Riegger G, Camm AJ, Martinez FA, Bradstreet DC, Ikeda LS, Santoro EP, investigators ELITEII. Comparison of losartan and captopril on heart failure-related outcomes and symptoms from the losartan heart failure survival study (ELITE II). *Am Heart J* 150: 123–131, 2005.
17. Konstam MA, Rousseau MF, Kronenberg MW, Udelson JE, Melin J, Stewart D, Dolan N, Edens TR, Ahn S, Kinan D, Howe DM, Kilcoyne L, Metherall J, Benedict C, Yusuf S, Pouleur H, investigators SOLVD. Effects of the angiotensin converting enzyme inhibitor enalapril on the long-term progression of left ventricular dysfunction in patients with heart failure. *Circulation* 86: 431–438, 1992.
18. Lameris TW, de Zeeuw S, Duncker DJ, Alberts G, Boomsma F, Verdouw PD, van den Meiracker AH. Exogenous angiotensin II does not facilitate norepinephrine release in the heart. *Hypertension* 40: 491–497, 2002.
19. Li M, Zheng C, Sato T, Kawada T, Sugimachi M, Sunagawa K. Vagal nerve stimulation markedly improves long-term survival after chronic heart failure in rats. *Circulation* 109: 120–124, 2004.
20. Nakayama Y, Miyano H, Shishido T, Inagaki M, Kawada T, Sugimachi M, Sunagawa K. Heart rate-independent vagal effect on end-systolic elastance of the canine left ventricle under various levels of sympathetic tone. *Circulation* 104: 2277–2279, 2001.
21. Paul M, Mehr AP, Kreutz R. Physiology of local renin-angiotensin systems. *Physiol Rev* 86: 747–803, 2006.
22. Peach MJ. Renin-angiotensin system: Biochemistry and mechanisms of action. *Physiol Rev* 57: 313–370, 1977.
23. Potter EK. Angiotensin inhibits action of vagus nerve at the heart. *Br J Pharmacol* 75: 9–11, 1982.
24. Qin Q, Downey JM, Cohen MV. Acetylcholine but not adenosine triggers preconditioning through PI3-kinase and a tyrosine kinase. *Am J Physiol Heart Circ Physiol* 284: H727–H734, 2003.
25. Rechtman M, Majewski H. A facilitatory effect of anti-angiotensin drugs on vagal bradycardia in the pithed rat and guinea-pig. *Br J Pharmacol* 110: 289–296, 1993.
26. Takata Y, Arai T, Suzuki S, Kurihara J, Uezono T, Okubo Y, Kato H. Captopril enhances cardiac vagal but not sympathetic neurotransmission in pithed rats. *J Pharmacol Sci* 95: 390–393, 2004.
27. Tune JD, Gorman MW, Feigl EO. Matching coronary blood flow to myocardial oxygen consumption. *J Appl Physiol* 97: 404–415, 2004.
28. van Kats JP, Danser AH, van Meegen JR, Sassen LM, Verdouw PD, Schalekamp MA. Angiotensin production by the heart. A quantitative study in pigs with the use of radiolabeled angiotensin infusions. *Circulation* 98: 73–81, 1998.
29. Yao Z, Gross GJ. Acetylcholine mimics ischemic preconditioning via a glibenclamide-sensitive mechanism in dogs. *Am J Physiol Heart Circ Physiol* 264: H2221–H2225, 1993.
30. Zhang C, Knudson JD, Setty S, Araiza A, Dincer üD, Kuo L, Tune JD. Coronary arteriolar vasoconstriction to angiotensin II is augmented in prediabetic metabolic syndrome via activation of AT₁ receptors. *Am J Physiol Heart Circ Physiol* 288: H2154–H2162, 2005.

Muscarinic potassium channels augment dynamic and static heart rate responses to vagal stimulation

Masaki Mizuno,¹ Atsunori Kamiya,¹ Toru Kawada,¹ Tadayoshi Miyamoto,^{1,2,3} Shuji Shimizu,^{1,2} and Masaru Sugimachi¹

¹Department of Cardiovascular Dynamics, Advanced Medical Engineering Center, National Cardiovascular Center Research Institute, and ³Morinomiyama University of Medical Sciences, Osaka; and ²Japan Association for the Advancement of Medical Equipment, Tokyo, Japan

Submitted 23 March 2007; accepted in final form 22 May 2007

Mizuno M, Kamiya A, Kawada T, Miyamoto T, Shimizu S, Sugimachi M. Muscarinic potassium channels augment dynamic and static heart rate responses to vagal stimulation. *Am J Physiol Heart Circ Physiol* 293: H1564–H1570, 2007. First published May 25, 2007; doi:10.1152/ajpheart.00368.2007.—Vagal control of heart rate (HR) is mediated by direct and indirect actions of ACh. Direct action of ACh activates the muscarinic K⁺ (K_{ACh}) channels, whereas indirect action inhibits adenylyl cyclase. The role of the K_{ACh} channels in the overall picture of vagal HR control remains to be elucidated. We examined the role of the K_{ACh} channels in the transfer characteristics of the HR response to vagal stimulation. In nine anesthetized sino-aortic-denervated and vagotomized rabbits, the vagal nerve was stimulated with a binary white-noise signal (0–10 Hz) for examination of the dynamic characteristic and in a step-wise manner (5, 10, 15, and 20 Hz/min) for examination of the static characteristic. The dynamic transfer function from vagal stimulation to HR approximated a first-order, low-pass filter with a lag time. Tertiapin, a selective K_{ACh} channel blocker (30 nmol/kg iv), significantly decreased the dynamic gain from 5.0 ± 1.2 to 2.0 ± 0.6 (mean \pm SD) beats \cdot min⁻¹ \cdot Hz⁻¹ ($P < 0.01$) and the corner frequency from 0.25 ± 0.03 to 0.06 ± 0.01 Hz ($P < 0.01$) without changing the lag time (0.37 ± 0.04 vs. 0.39 ± 0.05 s). Moreover, tertiapin significantly attenuated the vagal stimulation-induced HR decrease by 46 ± 21 , 58 ± 18 , 65 ± 15 , and $68 \pm 11\%$ at stimulus frequencies of 5, 10, 15, and 20 Hz, respectively. We conclude that K_{ACh} channels contribute to a rapid HR change and to a larger decrease in the steady-state HR in response to more potent tonic vagal stimulation.

systems analysis; transfer function; muscarinic receptor; rabbit

VAGAL CONTROL OF HEART RATE (HR) is mediated by a cascade reaction to ACh release. ACh binds to M₂ muscarinic receptors and, consequently, decreases HR. However, the pathway is not simple; two different pathways mediate the ACh-induced HR decrease. The M₂ muscarinic receptors activate heterotrimeric G_i and/or G_o proteins in cardiac myocytes (18); the action of ACh is determined by the G_i protein subunits. Via a direct pathway, a G_i protein $\beta\gamma$ -subunit activates inwardly rectifying muscarinic K⁺ (K_{ACh}) channels in the sinoatrial node cells (11, 28, 35); K_{ACh} channels then exert a negative chronotropic effect by hyperpolarizing the sinoatrial node cells. On the other hand, via an indirect pathway, a G_i protein α -subunit suppresses adenylyl cyclase (12, 32); the suppression of adenylyl cyclase then decreases HR by inhibiting inward currents in the sinoatrial node cells, which are activated by cAMP or cAMP-

dependent protein kinase. However, functional roles of the direct and indirect actions of ACh are not fully understood in the overall picture of vagal control of HR.

As a function in the dual control of adenylyl cyclase by G protein (12), the indirect action of ACh counteracts the G_s proteins activated by β_1 -adrenergic sympathetic stimulation and relies on slower changes in intracellular cAMP levels (8). On the contrary, the direct action of ACh utilizes the faster membrane-delimited mechanisms involving K_{ACh} channels (3) and is believed to be independent of sympathetic control. Given the rapidity of vagal HR control compared with sympathetic control (2, 14, 31), we hypothesized that the direct action of ACh via K_{ACh} channels contributes to the quickness of the vagal HR control in vivo. To test this hypothesis, we used the selective K_{ACh} channel blocker tertiapin to examine the dynamic and static transfer characteristics of the HR response to vagal stimulation (7, 10, 13, 15).

The pioneering work by Yamada (34) demonstrated that the direct action of ACh via K_{ACh} channels mediates ~75% of the steady-state negative chronotropic effects relative to the maximum carbachol-induced bradycardia in the isolated rabbit heart (i.e., static HR response to vagal stimulation). However, in this study, the role of K_{ACh} channels in the dynamic HR response to vagal stimulation was not analyzed quantitatively. Because HR changes dynamically in response to daily activities, quantification of dynamic and static characteristics is equally important. For instance, information on the dynamic HR response is key to understanding the generation of HR variability. Berger et al. (2) used transfer function analysis to identify the dynamic characteristics of the HR response. Saul et al. (29) demonstrated the utility of transfer function analysis for insight into cardiovascular regulation. The present study aims to expand our knowledge of the involvement of K_{ACh} channels in dynamic HR control by the vagal system.

MATERIALS AND METHODS

Surgical preparations. Animal care was consistent with the "Guiding Principles for Care and Use of Animals in the Field of Physiological Sciences," of the Physiological Society of Japan. All protocols were reviewed and approved by the Animal Subjects Committee of the National Cardiovascular Center. Nine Japanese White rabbits (2.5–3.2 kg body wt) were anesthetized by a mixture of urethane (250 mg/ml) and α -chloralose (40 mg/ml): initiation with a bolus injection of 2 ml/kg and maintenance with continuous administration at 0.5

Address for reprint requests and other correspondence: M. Mizuno, Dept. of Cardiovascular Dynamics, Advanced Medical Engineering Center, National Cardiovascular Center Research Institute, 5-7-1 Fujishirodai, Suita, Osaka 565-8565, Japan (e-mail: m-mizuno@ri.ncvc.go.jp).

The costs of publication of this article were defrayed in part by the payment of page charges. The article must therefore be hereby marked "advertisement" in accordance with 18 U.S.C. Section 1734 solely to indicate this fact.

ml·kg⁻¹·h⁻¹. The rabbits were intubated and mechanically ventilated with oxygen-enriched room air. Arterial pressure (AP) was measured by a micromanometer (model SPC-330A, Millar Instruments, Houston, TX) inserted into the right femoral artery and advanced to the thoracic aorta. HR was measured with a cardiometer (model N4778, San-ei, Tokyo, Japan). A double-lumen catheter was introduced into the right femoral vein for continuous anesthetic and drug administration. Sinoaortic denervation was performed bilaterally to minimize changes in the sympathetic efferent nerve activity via arterial baroreflexes. Bilateral section of the cardiac postganglionic sympathetic nerves minimized any possible interaction between the vagus and sympathetic nerves. The vagi were sectioned bilaterally at the neck. A pair of bipolar electrodes were attached to the cardiac end of the sectioned right vagus for vagal stimulation. Immersion of the stimulation electrodes and nerves in a mixture of white petroleum jelly (Vaseline) and liquid paraffin prevented drying and provided insulation. Body temperature was maintained at 38°C with a heating pad throughout the experiment.

Experimental procedures. The pulse duration of nerve stimulation was set at 2 ms. The stimulation amplitude of the right vagus was adjusted to yield an HR decrease of ~50 beats/min at a stimulation frequency of 10 Hz. After this adjustment, the amplitude of vagal stimulation was fixed at 1.8–6.0 V. Initiation of vagal nerve stimulation over 1 h upon completion of surgical preparations allowed stable hemodynamics. A preliminary examination indicated that the response of HR to vagal stimulation was stable for up to 3 h in our experimental settings (10 min of dynamic vagal stimulation at 50-min intervals; data not shown).

Dynamic protocol. For estimation of the dynamic transfer characteristics from vagal stimulation to HR response, the right vagus was stimulated by a frequency-modulated pulse train for 10 min. The stimulation frequency was switched every 500 ms at 0 or 10 Hz according to a binary white-noise signal. The power spectrum of the stimulation signal was reasonably constant up to 1 Hz. The transfer function was estimated up to 1 Hz, because the reliability of estimation decreased as a result of the diminution of input power above this frequency. The selected frequency range sufficiently spanned the physiological range of interest with respect to the dynamic vagal control of HR.

Static protocol. For estimation of the static transfer characteristics from vagal stimulation to HR response, step-wise vagal stimulation was performed. Vagal stimulation frequency was increased from 5 to 20 Hz in 5-Hz increments. Each frequency step was maintained for 60 s.

The dynamic and static transfer functions from vagal stimulation to HR response were estimated under control and K_{ACH} channel blockade conditions. After the control data were recorded, a bolus injection (30 nmol/kg iv) of a selective K_{ACH} channel blocker, tertiapin (Peptide Institute, Osaka, Japan), was administered, and vagal stimulation protocols were repeated 15 min thereafter. The control data were obtained first in all animals, because the long-lasting (>2 h) effects of tertiapin (data not shown) did not permit the subsequent acquisition of control data. A >5-min interval between dynamic and step-wise stimulation protocols confirmed that AP and HR returned to baseline levels. Dynamic and step-wise vagal stimulation protocols were randomly assigned under control and K_{ACH} channel blockade conditions.

β-Adrenergic blockade protocol. A supplemental experiment was performed under β-adrenergic blockade (*n* = 3) eliminated any effect of sympathetic activity. At ~10 min after a bolus injection of propranolol (1 mg/kg iv) (22), HR and AP reached a new steady state. The dynamic and static transfer functions from vagal stimulation to HR response were estimated before and after tertiapin treatment, both under β-adrenergic blockade.

Data analysis. A 12-bit analog-to-digital converter was used to digitize data at 200 Hz, and data were stored on the hard disk of a dedicated laboratory computer system. The dynamic transfer function from binary white-noise vagal stimulation to HR response was esti-

mated as follows. Input-output data pairs of the vagal stimulation frequency and HR were resampled at 10 Hz; then data pairs were partitioned into eight 50%-overlapping segments consisting of 1,024 data points each. For each segment, the linear trend was subtracted, and a Hanning window was applied. A fast Fourier transform was then performed to obtain the frequency spectra for vagal stimulation $[N(f)]$ and HR $[HR(f)]$ (4). Over the eight segments, the power of vagal stimulation $[S_{N \cdot N}(f)]$, the power of HR $[S_{HR \cdot HR}(f)]$, and the cross power between these two signals $[S_{N \cdot HR}(f)]$ were ensemble averaged. Finally, the transfer function $[H(f)]$ from vagal stimulation to the HR response was determined as follows (1, 20)

$$H(f) = \frac{S_{N \cdot HR}(f)}{S_{N \cdot N}(f)} \quad (1)$$

The transfer function from vagal stimulation to HR response approximated a first-order, low-pass filter with a lag time in previous studies (14, 21–24); therefore, the estimated transfer function was parameterized as follows

$$H(f) = \frac{-K}{1 + \frac{f}{f_c} j} e^{-2\pi f j L} \quad (2)$$

where *K* represents the dynamic gain (or, more precisely, the steady-state gain, in beats·min⁻¹·Hz⁻¹), *f_c* denotes the corner frequency (in Hz), *L* denotes the lag time (in s), and *f* and *j* represent frequency and the imaginary unit, respectively. The negative sign in the numerator indicates the negative HR response to vagal stimulation. The steady-state gain indicates the asymptotic value of the relative amplitude of the HR response to vagal nerve stimulation obtained in the frequency of input modulation approaching zero. The corner frequency represents the frequency of input modulation at which gain decreases by 3 dB from the steady-state gain in the frequency domain and reflects the readiness of the HR response for vagal stimulation in the time domain. The dynamic gain, corner frequency, and lag time were estimated by an iterative nonlinear least-squares regression. The phase shift of the transfer function indicates, with respect to the input signal, a lag or lead in the output signal normalized by its corresponding frequency of input modulation.

To quantify the linear dependence of the HR response on vagal stimulation, the magnitude-squared coherence function $[Coh(f)]$ was estimated as follows (1, 20)

$$Coh(f) = \frac{|S_{N \cdot HR}(f)|^2}{S_{N \cdot N}(f) \cdot S_{HR \cdot HR}(f)} \quad (3)$$

Coherence values range from zero to unity. Unity coherence indicates perfect linear dependence between the input and output signals; in contrast, zero coherence indicates total independence between the two signals.

To facilitate the intuitive understanding of the system dynamic characteristics, we calculated the system step response of HR to 1-Hz nerve stimulation as follows. The system impulse response was derived from the inverse Fourier transform of $H(f)$. The system step response was then obtained from the time integral of the impulse response. The length of the step response was 51.2 s. We calculated the maximum step response by averaging the last 10 s of the step response. The 90% rise time of the step response was determined as the time required for the response to reach 90% of the maximum step response. The time constant of the step response was calculated from the corner frequency of the corresponding transfer function as follows

$$\text{time constant} = \frac{1}{2 \cdot \pi \cdot f_c} \quad (4)$$

where the time constant is related inversely to the corner frequency without influence of the lag time.

The static transfer function from step-wise vagal stimulation to HR was estimated by averaging the HR data during the final 10 s of the 60-s stimulation at each stimulation frequency.

Statistical analysis. Values are means ± SD. Student's paired *t*-test was used to test differences in fitted parameters and calculated step response between control and K_{ACH} channel blockade conditions. For hemodynamic parameters, a two-way ANOVA, with drug and vagal stimulation as the main effects, was used to determine significant differences. For percent reduction from the control conditions in each parameter, one-way ANOVA was used to determine significant differences. *P* < 0.05 was considered significant.

RESULTS

Dynamic characteristics. Figure 1A shows typical recordings and corresponding power spectra of vagal stimulation and HR response under control and K_{ACH} channel blockade conditions. Random vagal stimulation decreased HR intermittently. Tertiapin-mediated K_{ACH} channel blockade attenuated the amplitude of the variation and the speed of the HR response to vagal stimulation. In the power spectral plot, tertiapin decreased the HR power. The decrease in the HR power was

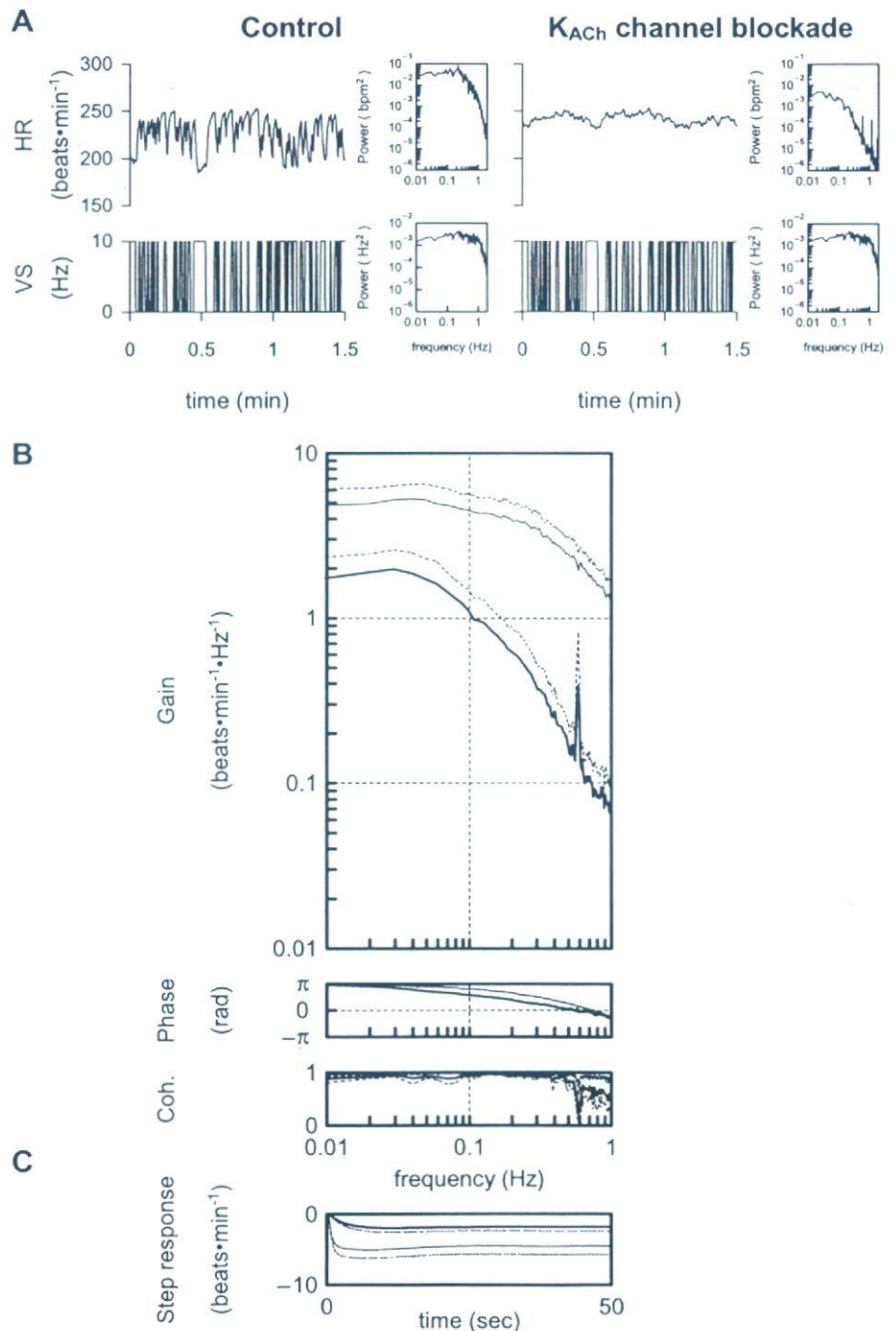


Fig. 1. *A*: representative recordings of heart rate (HR) obtained utilizing binary white-noise vagal stimulation (*top*) and corresponding vagal stimulation (VS, *bottom*). Traces were recorded before (control, *left*) and after tertiapin infusion (30 nmol/kg iv) for muscarinic K⁺ (K_{ACH}) channel blockade (*right*). *Insets*: power spectra of each parameter. Tertiapin attenuated amplitude of HR variation and speed of response of HR to vagal stimulation. *B*: dynamic transfer function relating vagal stimulation to HR responses averaged from all animals (pooled data, *n* = 9). *Top*: gains; *middle*: phase shifts; *bottom*: coherence (Coh) functions. Frequency on abscissa (gain and phase) indicates frequency of input modulation, rather than stimulation frequency. *C*: calculated step response to 1-Hz tonic vagal stimulation averaged from all animals (pooled data, *n* = 9). Solid lines, means; dashed lines, SD. Thin line, control; thick line, K_{ACH} channel blockade with tertiapin (30 nmol/kg iv). Tertiapin decreased transfer gain and increased phase shift with increasing frequency, and tertiapin decreased maximum step response and slowed initial step response.

Table 1. Effects of tertiapin infusion on AP and HR before and during dynamic vagal stimulation

	Control	Tertiapin
AP, mmHg		
Before stimulation	82.4 ± 20.5	77.6 ± 20.7
During stimulation	77.9 ± 20.0	74.8 ± 18.6
HR, beats/min		
Before stimulation	247.3 ± 24.7	248.1 ± 32.7
During stimulation	212.4 ± 22.3	231.1 ± 25.9

Values are means ± SD ($n = 9$). Tertiapin was infused at 30 nmol/kg iv. AP, arterial pressure; HR, heart rate. Vagal stimulation significantly decreased HR ($P < 0.01$), but no significant effect of drug ($P = 0.28$) or interaction ($P = 0.32$) was observed by 2-way ANOVA.

more potent in the higher (>0.1 Hz) than in the lower frequency range.

Table 1 summarizes the mean values of AP and HR before and during vagal stimulation averaged from all animals. Dynamic vagal stimulation significantly decreased the mean HR ($P < 0.01$), but not the mean AP. Tertiapin did not significantly affect mean AP or HR before or during stimulation.

Figure 1B illustrates the dynamic transfer functions characterizing the vagal HR response averaged from all animals under control and tertiapin-mediated K_{ACh} channel blockade conditions. Gain plots, phase plots, and coherence functions are shown. Tertiapin attenuated the dynamic gain compared with the control conditions; the extent of the attenuation was greater in the higher frequency range: 63.0 ± 11.6 , 74.4 ± 8.3 , 93.0 ± 2.5 , and $93.3 \pm 3.9\%$ at 0.01, 0.1, 0.5, and 1 Hz, respectively, as normalized to the control condition ($P < 0.01$ by ANOVA). The peak in the gain at 0.6 Hz observed during tertiapin-mediated K_{ACh} channel blockade would be caused by the artificial respiration (respiratory rate = 35–40 min⁻¹), because the low coherence value (~ 0.1) at 0.6 Hz indicates the independence of the input and output signals. This peak was masked by the large HR response to vagal stimulation under the control condition. The phase approached π radians at the lowest frequency and lagged with increasing frequency under the control condition; tertiapin caused the phase difference between the two conditions in the frequency range of 0.03–0.7 Hz, which disappeared at 1 Hz. The fitted parameters of the transfer functions are summarized in Table 2. Tertiapin significantly decreased the dynamic gain and the corner frequency without changing the lag time. Coherence was near unity in the overall frequency range in the control condition, whereas a decrease in the coherence function from unity was noted at >0.6 Hz with K_{ACh} channel blockade.

Figure 1C shows the calculated step response of HR to vagal stimulation averaged from all animals in the control condition and during K_{ACh} channel blockade. Tertiapin slowed the transient response (time constants = 0.6 ± 0.1 to 2.7 ± 0.5 s, $P < 0.01$) and attenuated the HR response to vagal stimulation (maximum step response = -4.5 ± 1.2 to -1.8 ± 0.6 beats/min, $P < 0.01$) in the time domain. Furthermore, tertiapin significantly delayed the 90% rise time of the step response, which was calculated as an index of system readiness (1.6 ± 0.5 to 5.0 ± 1.4 s, $P < 0.01$).

Static characteristics. Figure 2A shows typical recordings of step-wise vagal stimulation and the HR response in the control condition and during K_{ACh} channel blockade. The step-wise

vagal stimulation decreased HR in a step-wise manner. Tertiapin attenuated the static reductions of HR from the baseline HR.

Figure 2B summarizes changes in HR in response to step-wise vagal stimulation. The step-wise vagal stimulation significantly decreased HR with increasing stimulus frequency under both conditions. Tertiapin significantly attenuated the static reductions of HR. The attenuation of HR reduction normalized to control conditions increased with increasing stimulus frequency: 45.8 ± 21.3 , 58.2 ± 17.9 , 64.7 ± 14.6 , and $68.0 \pm 11.4\%$ at 5, 10, 15, and 20 Hz, respectively ($P < 0.05$ by ANOVA).

β -Adrenergic blockade protocol. In the supplemental protocol ($n = 3$) with β -adrenergic blockade, tertiapin decreased the dynamic gain from 2.4 ± 0.6 to 1.3 ± 0.5 beats·min⁻¹·Hz⁻¹ and the corner frequency from 0.23 ± 0.05 to 0.06 ± 0.02 Hz without changing the lag time (0.36 ± 0.01 vs. 0.43 ± 0.00 s). In terms of the static characteristics, tertiapin significantly attenuated the vagal stimulation-induced HR decrease by 43 ± 10, 50 ± 8, 56 ± 7, and 61 ± 8% at stimulus frequencies of 5, 10, 15, and 20 Hz, respectively.

DISCUSSION

We have quantified the role of the K_{ACh} channels by examining the transfer characteristics. The major findings in the present study are that K_{ACh} channel blockade with intravenous tertiapin administration decreased the dynamic gain and corner frequency without changing the lag time of the dynamic transfer function from vagal stimulation to HR. These findings support our hypothesis that direct action of ACh via K_{ACh} channels contributes to the quickness of the HR control in response to electrical vagal stimulation.

Effect of tertiapin on dynamic transfer characteristics. Our results indicate that K_{ACh} channels contribute to a rapid component in vagal HR control. Tertiapin slowed the dynamic HR response to vagal stimulation, since tertiapin attenuated the gain of the transfer function significantly in the high frequency range (Fig. 1B). Moreover, the calculated step response clearly demonstrated this point (Fig. 1C). Tertiapin prolonged the time constant and 90% rise time of the step response by 2.1 and 3.4 s, respectively. Since quickness is a hallmark of the vagal control of HR relative to sympathetic control, these results highlight the importance of K_{ACh} channels in the rapidity of vagal HR control. Because tertiapin did not affect the lag time (Table 2), the increase in the 90% rise time to the step response due to tertiapin (~ 3.4 s) may primarily reflect the slowed transient response.

Our results are consistent with and may partly explain the earlier studies in which transgenic mice were used to investigate the role of K_{ACh} channels (8, 33). Using the G protein-

Table 2. Effects of tertiapin infusion on parameters of the transfer function relating dynamic vagal stimulation to HR

	Control	Tertiapin
Dynamic gain, beats·min ⁻¹ ·Hz ⁻¹	5.0 ± 1.2	2.0 ± 0.6*
Corner frequency, Hz	0.25 ± 0.03	0.06 ± 0.01*
Lag time, s	0.37 ± 0.04	0.39 ± 0.05

Values are means ± SD. Tertiapin was infused at 30 nmol/kg iv. * $P < 0.01$ vs. corresponding control.

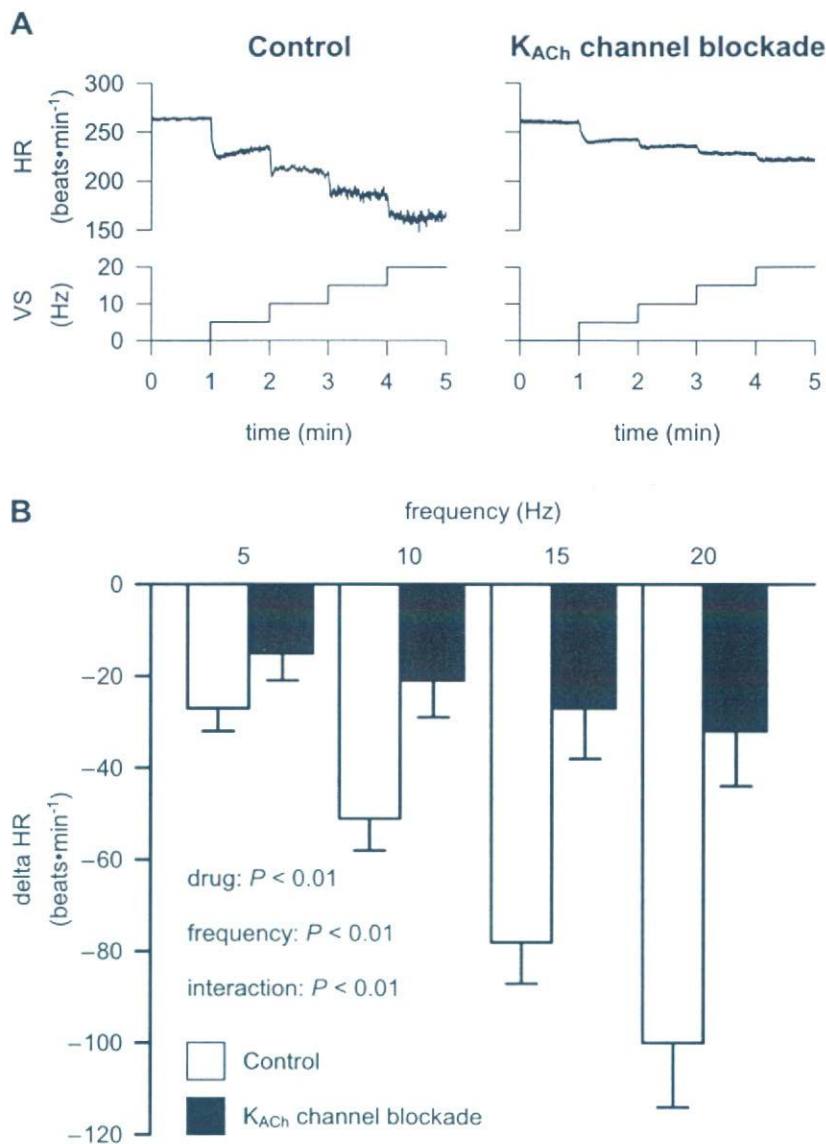


Fig. 2. *A*: representative recordings of HR (*top*) and corresponding vagal stimulation (*bottom*) obtained utilizing a step-wise stimulation. Traces were recorded before (control, *left*) and after tertiapin infusion (30 nmol/kg iv) for K_{ACh} channel blockade (*right*). K_{ACh} channel blockade attenuated amplitude of HR variation to tonic vagal stimulation. *B*: static transfer function relating step-wise vagal stimulation to HR responses averaged from all animals (pooled data, $n = 9$). Basal HR was not different between control and K_{ACh} channel blockade (see Table 1). K_{ACh} channel blockade decreases static HR response, and static reductions in bradycardic effect were greater at higher stimulation frequencies.

gated inwardly rectifying potassium (GIRK) channel family subunit GIRK4, which is a component of K_{ACh} channels (5, 16), Wickman et al. (33) indicated that the spectral power of HR was lower at 1.5–5.0 Hz, which is predominantly vagally mediated, but not at <0.4 Hz, in GIRK4-knockout than in wild-type mice. Another study using transgenic mice with a reduction in functional $\beta\gamma$ -subunits of the G_i proteins also showed impaired vagal HR control, such as reductions in carbachol-induced bradycardia, HR variability, and baroreflex sensitivity (8). In the present study, tertiapin significantly attenuated the dynamic gain compared with the control conditions in the frequency bands from 0.01 to 1 Hz; the extent of the decreases in dynamic gain was augmented with increasing frequency of input modulation. This finding also supports the notion that K_{ACh} channels play a large part as a rapid component of vagal control of HR. Furthermore, increased phase shift due to tertiapin in the higher frequency range (0.03–0.7 Hz) would support the interpretation that the K_{ACh} channel current played an important role in the rapid HR response to vagal stimulation.

Tertiapin-mediated changes in fitted parameters of the transfer function from vagal stimulation to HR suggest that, at the postjunctional effector sites, the K_{ACh} channels play a key role in determining the dynamic properties of transduction from vagal nerve activity to HR. To quantitatively elucidate vagal and sympathetic control of HR, our research group used a transfer function analysis to examine the system characteristics. First, the transfer function from dynamic vagal nerve stimulation to HR approximated the characteristics of a first-order, low-pass filter, whereas the transfer function from dynamic sympathetic nerve stimulation to HR approximated the characteristics of a second-order, low-pass filter (14). Dynamic gain of vagal stimulation to HR was increased by concomitant sympathetic nerve stimulation (14) and pharmacologically induced accumulation of cAMP at the postjunctional effector sites (23) and decreased by high plasma norepinephrine (21). These perturbations of the indirect action of ACh did not affect the quickness of vagal HR control; i.e., neither corner frequency nor lag time was altered. On the contrary, inhibition of cholinesterase by neostigmine decreased the corner frequency

and increased the lag time (24). Taken together, these results might suggest that not only ACh kinetics at the neuroeffector site, but also the K_{ACh} channels at the postjunctional effector sites, play a key role in determining the dynamic properties of transduction from vagal nerve activity to HR.

Effect of tertiapin on the static transfer characteristics. Tertiapin attenuates the static reduction of HR in accord with the attenuation of the gain of the dynamic transfer function at the lowest frequency of input modulation. This suggests that K_{ACh} channels contribute to the static, as well as the rapid, component of vagal HR control. The relative attenuation of HR reduction increased with increasing stimulus frequency (Fig. 2B), suggesting that direct action of ACh in the static properties of transduction from vagus nerve activity to HR is augmented by an increase in the amount of available ACh. Although it is well established that the muscarinic response to static vagal stimulation depends on the stimulation frequency (26, 27), whether the contribution of the K_{ACh} channel pathway to the total HR response depends on the stimulus frequency remains unknown. The basal mean HR of GIRK-knockout mice (33) and transgenic mice with a reduction of $\beta\gamma$ -subunits of the G_i proteins (8) is the same as that of wild-type mice, suggesting that K_{ACh} channels are not involved in mean HR control in the basal state. At low-to-moderate levels of vagal activity, vagal control of HR is due to changes in cAMP-modulated I_h , often referred to as "pacemaker" current (6). K_{ACh} channels might play an essential role in HR control at high levels of vagal activity.

In the present study, tertiapin decreased the HR response to vagal stimulation by ~70% of the control condition at a stimulus intensity of 20 Hz. This value is consistent with the earlier study by Yamada (34). This consistency suggested that K_{ACh} channels contribute to ~70% of the maximum negative chronotropic effects to pharmacologically and/or electronically induced vagal stimulation. However, changes in HR induced by tertiapin may have in turn affected the indirect action of ACh in the present study. Therefore, the percentage of direct vs. indirect action should be carefully interpreted.

Limitations. There are several limitations to this study. First, we did not confirm the completeness of K_{ACh} channel blockade. Kitamura et al. (15) demonstrated that tertiapin potently and selectively blocked the K_{ACh} channel in cardiac myocytes in a muscarinic receptor- and voltage-independent manner. Furthermore, Drici et al. (7) showed that tertiapin blocked K_{ACh} channels with an IC₅₀ of ~30 nM with no significant effect on major currents associated with the cardiac repolarization process or atrioventricular conduction. On the basis of these studies, Hashimoto et al. (10) demonstrated that tertiapin (12 nmol/kg iv) significantly prolonged the atrial effective refractory period during vagal stimulation in their in vivo canine study. Therefore, we believe that the dose of tertiapin (30 nmol/kg iv) used in the present study should be sufficient to block K_{ACh} channel current in vivo.

Second, data were obtained from anesthetized animals. Since the anesthesia would affect the autonomic tone, the results may not be directly applicable to conscious animals. However, because we cut and stimulated the right cardiac vagal nerve, changes in autonomic outflow associated with anesthesia might not have significantly affected the results.

Third, in the present study, we stimulated the vagal nerve according to binary white noise and a step-wise pattern, which

was quite different from the pattern of physiological neuronal discharge. However, although nonphysiological patterns of stimulation could theoretically bias the system identification results, because coherence was near unity over the frequency range of interest, by virtue of their inherent linearity, the system properties would not vary much with differing patterns of stimulation.

In conclusion, K_{ACh} channel blockade with intravenous tertiapin administration decreased the dynamic gain and corner frequency without changing the lag time of the transfer function from vagal stimulation to HR. In the time domain, tertiapin prolonged the time constant and 90% rise time of the step response. Additionally, tertiapin decreased the static reductions of HR from baseline HR to less than half of the control response with increasing vagal stimulus frequency. These results suggest that K_{ACh} channels accelerate the dynamic HR response to vagal stimulation and contribute more to the static HR response for more potent tonic vagal stimulation in vivo.

Perspectives

To simply identify the role of K_{ACh} channels in vagal HR control, a previous study (34) and the present study completely and/or partially excluded background sympathetic tone. However, in the physiological condition, sympathetic tone affects vagal control of HR and vice versa [e.g., accentuated antagonism (17)]. Pathophysiological conditions such as chronic heart failure (25), hypertension (19), and obesity (30) reveal increased basal sympathetic nerve activity compared with the normal condition. Tertiapin did not affect basal AP or HR (Table 1), suggesting that tertiapin did not affect sympathetic tone in the present experimental settings. Furthermore, under β -adrenergic blockade (the supplemental protocol), tertiapin decreased the dynamic gain and corner frequency, suggesting that the effects of tertiapin cannot be explained by the background sympathetic tone. However, the experimental design of the present study did not allow separate assessment of the direct vs. the indirect action of ACh, because the indirect action of ACh was not manipulated intentionally. Further investigation is needed to clarify the effects of sympathetic tone on the contribution of K_{ACh} channels to negative chronotropic effects.

GRANTS

This study was supported by Health and Labour Sciences Research Grants H15-Physi-001, H18-Nano-Ippan-003, and H18-Iryo-Ippan-023 from the Ministry of Health, Grant-in-Aid for Scientific Research promoted by the Ministry of Education, Culture, Sports, Science and Technology in Japan 18591992, and the Ground-Based Research Announcement for Space Utilization project promoted by the Japan Space Forum. This study was also supported by Industrial Technology Research Program Grant 06B44524a from the New Energy and Industrial Technology Development Organization of Japan.

REFERENCES

1. Bendat J, Piersol A. Single-input/output relationships. In: *Random Data Analysis and Measurement Procedures* (3rd ed). New York: Wiley, 2000, p. 189–217.
2. Berger RD, Saul JP, Cohen RJ. Transfer function analysis of autonomic regulation. I. Canine atrial rate response. *Am J Physiol Heart Circ Physiol* 256: H142–H152, 1989.
3. Breitwieser GE, Szabo G. Uncoupling of cardiac muscarinic and β -adrenergic receptors from ion channels by a guanine nucleotide analogue. *Nature* 317: 538–540, 1985.
4. Brigham E. FFT transform application. In: *The Fast Fourier Transform and Its Application*. Englewood Cliffs, NJ: Prentice-Hall, 1988, p. 167–203.

5. Dascal N, Schreibley W, Lim NF, Wang W, Chavkin C, DiMagno L, Labarca C, Kieffer BL, Gaveriaux-Ruff C, Trollinger D, Lester HA, Davidson N. Atrial G protein-activated K⁺ channel: expression, cloning, and molecular properties. *Proc Natl Acad Sci USA* 90: 10235–10239, 1993.
6. DiFrancesco D. Cardiac pacemaker: 15 years of “new” interpretation. *Acta Cardiol* 50: 413–427, 1995.
7. Drici MD, Diochot S, Terrenoire C, Romey G, Lazdunski M. The bee venom peptide tertiapin underlines the role of I_{KACH} in acetylcholine-induced atrioventricular blocks. *Br J Pharmacol* 131: 569–577, 2000.
8. Gehrmann J, Meister M, Maguire CT, Martins DC, Hammer PE, Neer EJ, Berul CI, Mende U. Impaired parasympathetic heart rate control in mice with a reduction of functional G protein βγ-subunits. *Am J Physiol Heart Circ Physiol* 282: H445–H456, 2002.
9. Hartzell HC, Mery PF, Fischmeister R, Szabo G. Sympathetic regulation of cardiac calcium current is due exclusively to cAMP-dependent phosphorylation. *Nature* 351: 573–576, 1991.
10. Hashimoto N, Yamashita T, Tsuruzoe N. Tertiapin, a selective I_{KACH} blocker, terminates atrial fibrillation with selective atrial effective refractory period prolongation. *Pharmacol Res* 54: 136–141, 2006.
11. Huang CL, Slesinger PA, Casey PJ, Jan YN, Jan LY. Evidence that direct binding of Gβγ to the GIRK1 G protein-gated inwardly rectifying K⁺ channel is important for channel activation. *Neuron* 15: 1133–1143, 1995.
12. Irisawa H, Brown HF, Giles W. Cardiac pacemaking in the sinoatrial node. *Physiol Rev* 73: 197–227, 1993.
13. Jin W, Lu Z. Synthesis of a stable form of tertiapin: a high-affinity inhibitor for inward-rectifier K⁺ channels. *Biochemistry* 38: 14286–14293, 1999.
14. Kawada T, Ikeda Y, Sugimachi M, Shishido T, Kawaguchi O, Yamazaki T, Alexander J Jr, Sunagawa K. Bidirectional augmentation of heart rate regulation by autonomic nervous system in rabbits. *Am J Physiol Heart Circ Physiol* 271: H288–H295, 1996.
15. Kitamura H, Yokoyama M, Akita H, Matsushita K, Kurachi Y, Yamada M. Tertiapin potently and selectively blocks muscarinic K⁺ channels in rabbit cardiac myocytes. *J Pharmacol Exp Ther* 293: 196–205, 2000.
16. Krapivinsky G, Gordon EA, Wickman K, Velimirovic B, Krapivinsky L, Clapham DE. The G-protein-gated atrial K⁺ channel I_{KACH} is a heteromultimer of two inwardly rectifying K⁺-channel proteins. *Nature* 374: 135–141, 1995.
17. Levy MN. Sympathetic-parasympathetic interactions in the heart. *Circ Res* 29: 437–445, 1971.
18. Luetje CW, Tietje KM, Christian JL, Nathanson NM. Differential tissue expression and developmental regulation of guanine nucleotide binding regulatory proteins and their messenger RNAs in rat heart. *J Biol Chem* 263: 13357–13365, 1988.
19. Mancica G, Grassi G, Giannattasio C, Seravalle G. Sympathetic activation in the pathogenesis of hypertension and progression of organ damage. *Hypertension* 34: 724–728, 1999.
20. Marmarelis P, Marmarelis V. The white noise method in system identification. In: *Analysis of Physiological Systems*. New York: Plenum, 1978, p. 131–221.
21. Miyamoto T, Kawada T, Takaki H, Inagaki M, Yanagiya Y, Jin Y, Sugimachi M, Sunagawa K. High plasma norepinephrine attenuates the dynamic heart rate response to vagal stimulation. *Am J Physiol Heart Circ Physiol* 284: H2412–H2418, 2003.
22. Miyamoto T, Kawada T, Yanagiya Y, Inagaki M, Takaki H, Sugimachi M, Sunagawa K. Cardiac sympathetic nerve stimulation does not attenuate dynamic vagal control of heart rate via α-adrenergic mechanism. *Am J Physiol Heart Circ Physiol* 287: H860–H865, 2004.
23. Nakahara T, Kawada T, Sugimachi M, Miyano H, Sato T, Shishido T, Yoshimura R, Miyashita H, Inagaki M, Alexander J Jr, Sunagawa K. Accumulation of cAMP augments dynamic vagal control of heart rate. *Am J Physiol Heart Circ Physiol* 275: H562–H567, 1998.
24. Nakahara T, Kawada T, Sugimachi M, Miyano H, Sato T, Shishido T, Yoshimura R, Miyashita H, Sunagawa K. Cholinesterase affects dynamic transduction properties from vagal stimulation to heart rate. *Am J Physiol Regul Integr Comp Physiol* 275: R541–R547, 1998.
25. Negro CE, Rondon MU, Tinucci T, Alves MJ, Roveda F, Braga AM, Reis SF, Nastari L, Barretto AC, Krieger EM, Middlekauff HR. Abnormal neurovascular control during exercise is linked to heart failure severity. *Am J Physiol Heart Circ Physiol* 280: H1286–H1292, 2001.
26. Parker P, Celler BG, Potter EK, McCloskey DI. Vagal stimulation and cardiac slowing. *J Auton Nerv Syst* 11: 226–231, 1984.
27. Priola DV, Cote I. Differential sensitivity of the canine heart to acetylcholine and vagal stimulation. *Am J Physiol Heart Circ Physiol* 234: H460–H464, 1978.
28. Sakmann B, Noma A, Trautwein W. Acetylcholine activation of single muscarinic K⁺ channels in isolated pacemaker cells of the mammalian heart. *Nature* 303: 250–253, 1983.
29. Saul JP, Berger RD, Albrecht P, Stein SP, Chen MH, Cohen RJ. Transfer function analysis of the circulation: unique insights into cardiovascular regulation. *Am J Physiol Heart Circ Physiol* 261: H1231–H1245, 1991.
30. Seals DR, Bell C. Chronic sympathetic activation: consequence and cause of age-associated obesity? *Diabetes* 53: 276–284, 2004.
31. Spear JF, Moore EN. Influence of brief vagal and stellate nerve stimulation on pacemaker activity and conduction within the atrioventricular conduction system of the dog. *Circ Res* 32: 27–41, 1973.
32. Sunahara RK, Dessauer CW, Gilman AG. Complexity and diversity of mammalian adenylyl cyclases. *Annu Rev Pharmacol Toxicol* 36: 461–480, 1996.
33. Wickman K, Nemecek J, Gendler SJ, Clapham DE. Abnormal heart rate regulation in GIRK4 knockout mice. *Neuron* 20: 103–114, 1998.
34. Yamada M. The role of muscarinic K⁺ channels in the negative chronotropic effect of a muscarinic agonist. *J Pharmacol Exp Ther* 300: 681–687, 2002.
35. Yamada M, Inanobe A, Kurachi Y. G protein regulation of potassium ion channels. *Pharmacol Rev* 50: 723–760, 1998.

Efferent vagal nerve stimulation induces tissue inhibitor of metalloproteinase-1 in myocardial ischemia-reperfusion injury in rabbit

Kazunori Uemura,¹ Meihua Li,¹ Takaki Tsutsumi,² Toji Yamazaki,³ Toru Kawada,¹ Atsunori Kamiya,¹ Masashi Inagaki,¹ Kenji Sunagawa,² and Masaru Sugimachi¹

Departments of ¹Cardiovascular Dynamics and ³Cardiac Physiology, National Cardiovascular Center Research Institute, Suita, Japan; and ²Department of Cardiovascular Medicine, Kyushu University Graduate School of Medical Science, Fukuoka, Japan

Submitted 24 April 2007; accepted in final form 7 August 2007

Uemura K, Li M, Tsutsumi T, Yamazaki T, Kawada T, Kamiya A, Inagaki M, Sunagawa K, Sugimachi M. Efferent vagal nerve stimulation induces tissue inhibitor of metalloproteinase-1 in myocardial ischemia-reperfusion injury in rabbit. *Am J Physiol Heart Circ Physiol* 293: H2254–H2261, 2007. First published August 10, 2007; doi:10.1152/ajpheart.00490.2007.—Vagal nerve stimulation has been suggested to ameliorate left ventricular (LV) remodeling in heart failure. However, it is not known whether and to what degree vagal nerve stimulation affects matrix metalloproteinase (MMP) and tissue inhibitor of MMP (TIMP) in myocardium, which are known to play crucial roles in LV remodeling. We therefore investigated the effects of electrical stimulation of efferent vagal nerve on myocardial expression and activation of MMPs and TIMPs in a rabbit model of myocardial ischemia-reperfusion (I/R) injury. Anesthetized rabbits were subjected to 60 min of left coronary artery occlusion and 180 min of reperfusion with (I/R-VS, $n = 8$) or without vagal nerve stimulation (I/R, $n = 7$). Rabbits not subjected to coronary occlusion with (VS, $n = 7$) or without vagal stimulation (sham, $n = 7$) were used as controls. Total MMP-9 protein increased significantly after left coronary artery occlusion in I/R-VS and I/R to a similar degree compared with VS and sham values. Endogenous active MMP-9 protein level was significantly lower in I/R-VS compared with I/R. TIMP-1 mRNA expression was significantly increased in I/R-VS compared with the I/R, VS, and sham groups. TIMP-1 protein was significantly increased in I/R-VS and VS compared with the I/R and sham groups. Cardiac microdialysis technique demonstrated that topical perfusion of acetylcholine increased dialysate TIMP-1 protein level, which was suppressed by co-perfusion of atropine. Immunohistochemistry demonstrated a strong expression of TIMP-1 protein in cardiomyocytes around the dialysis probe used to perfuse acetylcholine. In conclusion, in a rabbit model of myocardial I/R injury, vagal nerve stimulation induced TIMP-1 expression in cardiomyocytes and reduced active MMP-9.

myocardial remodeling; matrix metalloproteinase; acetylcholine

LEFT VENTRICULAR (LV) myocardial remodeling that occurs after myocardial infarction (MI) leads to progressive LV dilation and eventually pump dysfunction (33, 40). In addition to the loss of contractile cardiomyocytes, pathological degradation and reconstitution of extracellular matrix significantly contribute to the progression of LV remodeling, where matrix metalloproteinase (MMP) and its intrinsic inhibitor, tissue inhibitor of MMP (TIMP), play crucial roles (37, 43).

A previous study using genetically engineered mice demonstrated that target deletion of the MMP-9 gene prevented LV rupture and ameliorated LV remodeling after MI (10). The

positive results of MMP inhibition on LV remodeling in animal models led to the proposal to use MMP inhibitors as a potential therapy for patients at risk for the development of heart failure after MI (27, 32). However, recent clinical results from the Prevention of Myocardial Infarction Early Remodeling (PREMIER) trial failed to demonstrate a beneficial effect of MMP inhibition on LV remodeling after MI (16). This indicates the importance of further understanding the *in vivo* regulatory mechanisms of MMPs to understand and beneficially modify the LV remodeling process.

The cardiac autonomic nervous system plays an important role in the progression of heart failure (21). A previous communication from our laboratory demonstrated that chronic electrical stimulation of vagal nerve ameliorated LV remodeling and markedly improved survival after MI in rat (23). However, it is not known whether and to what degree the vagal nerve affects the MMPs and the TIMPs *in vivo*. We therefore investigated the effects of electrical stimulation of vagal nerve on myocardial expression of MMP-2/9 and TIMP-1/2 in a rabbit model of myocardial ischemia-reperfusion (I/R) injury. We also investigated the direct action of acetylcholine (ACh), a neurotransmitter released by vagal nerve stimulation (VNS), on myocardial release of TIMP-1 using a cardiac microdialysis technique (19). Our results indicated that VNS induced expression of TIMP-1 from cardiomyocytes and reduced active MMP-9 in myocardial I/R injury in rabbit.

METHODS

We used 49 Japanese white rabbits in this study (male, 2.5–3.0 kg). Care of the animals was in strict accordance with the guiding principles of the Physiological Society of Japan. All protocols were approved by the Animal Subjects Committee of the National Cardiovascular Center.

I/R Study

Experimental preparation. Anesthesia was induced by intravenous injection of pentobarbital sodium (35 mg/kg). Animals were tracheotomized, intubated, and mechanically ventilated. Arterial pH, P_{O_2} , and P_{CO_2} were maintained within the physiological ranges by supplying oxygen and changing the respiratory rate. α -Chloralose (20 mg·kg⁻¹·h⁻¹) was continuously infused to maintain an appropriate level of anesthesia during the experiment. A catheter-tipped micro-manometer (SPC-330A, Millar Instruments, Houston, TX) was inserted via the right femoral artery to measure arterial pressure (AP). After a median sternotomy, the heart was suspended in a pericardial

Address for reprint requests and other correspondence: K. Uemura, Dept. of Cardiovascular Dynamics, National Cardiovascular Center Research Inst., 5-7-1 Fujishirodai, Suita 565-8565, Japan (e-mail: kuemura@ri.nccvc.go.jp).

The costs of publication of this article were defrayed in part by the payment of page charges. The article must therefore be hereby marked "advertisement" in accordance with 18 U.S.C. Section 1734 solely to indicate this fact.

cradle. Another catheter-tipped micromanometer was introduced into the LV via the apex to measure LV pressure (LVP). Piezoelectric crystals (1 mm, Sonometrics, Ontario, Canada) were attached to the anterior and lateral walls of the LV using cyanoacrylate adhesive (3M, Vetbond, St. Paul, MN) to measure regional LV segmental length. A 4-0 prolene suture was passed around the main branch of the left anterior descending coronary artery (LAD), and a snare was formed by passing the ends of the thread through a small vinyl tube. A surface electrocardiogram (ECG) was recorded.

Bilateral cervical vagi were identified and transected at the neck region. A pair of bipolar electrodes was attached at the cardiac end of the right vagal nerve. The duration of electrical pulse used to stimulate the vagal nerve was set at 4 ms. We adjusted the amplitude of the pulse in each animal to reduce heart rate (HR) by 30% from the baseline value at a stimulation frequency of 10 Hz. The resultant stimulation voltage was 2–4 V.

Experimental protocol. Thirty minutes were allowed for stabilization after the initial preparation and surgical procedures were completed. The animals were randomized into the following four groups: 1) sham group ($n = 7$), in which surgical preparation was conducted without coronary occlusion or vagal stimulation (VS); 2) VS group ($n = 7$), in which stimulation of the vagal nerve was started after baseline hemodynamics were obtained and continued during the experiment; 3) I/R group ($n = 7$), in which 60 min of LAD occlusion and 180 min of reperfusion were conducted; and 4) I/R-VS group ($n = 8$), in which stimulation of the vagal nerve was started 15 min before LAD occlusion and continued throughout 60 min of myocardial ischemia and 180 min of reperfusion.

Baseline hemodynamic data (baseline) were recorded in all groups. A second set of measurements of hemodynamic data (60 min) was obtained during the last 5 min of the 60-min observation period in the sham and VS groups or during the last 5 min of the 60-min ischemic period in the I/R and I/R-VS groups. A third set of measurements of hemodynamic data (240 min) was recorded during the last 5 min of the next 180-min observation period in the sham and VS groups or during the last 5 min of the 180-min reperfusion period in the I/R and I/R-VS groups.

At each time point, hemodynamic data were recorded under a steady-state condition. All data acquisitions were done at end expiration. Analog signals of AP, LVP, segmental length of the anterior-lateral wall of LV (risk area), and ECG were digitized at 200 Hz and stored in a computer for off-line analysis (Sonolab, Sonometrics).

At the end of the experiment, the animal was euthanized. The whole heart was quickly excised and washed with cold PBS. After the vasculature, right ventricular free wall, and atrial appendages were dissected away, the remaining LV wall was snap frozen in liquid nitrogen and stored at -80°C .

Myocardial protein extraction. Approximately 200 mg of myocardial tissue sample obtained from the center of the risk area (anterior wall) of the LV free wall was homogenized in 1 ml of lysis buffer containing 50 mmol/l Tris (pH 7.4), 1.5 mmol/l CaCl_2 , and 0.5% Triton X-100. The homogenate was centrifuged at 2,000 g for 10 min at 4°C , and the supernatant was collected. Protein concentration of each supernatant sample was determined with a DC Protein assay kit (Bio-Rad, Richmond, CA).

Gelatin zymography. Gelatin zymography was performed to assess the relative contents of the gelatinases MMP-2 and MMP-9 (43). The supernatants (60 μg protein) were loaded in Novex precast 10% Tris-glycine gels containing 0.1% gelatin (Invitrogen, Carlsbad, CA) and then electrophoresed. After renaturation and equilibration, the gels were incubated for 30 h at 37°C in Novex zymogram-developing buffer. The gels were then stained in 0.5% Coomassie blue G-250, dissolved in 30% methanol-10% acetic acid for 60 min, and destained in several changes of methanol-acetic acid for 60 min. Gels were dried and scanned. MMP-2 and MMP-9 related bands were analyzed using the NIH Image software (ImageJ 1.37).

MMP-9 activity assay. Bioactivity assay for MMP-9 was performed using the Biotrak activity assay system (GE Healthcare Bio-Sciences, Piscataway, NJ) following the manufacturer's instructions (42). Briefly, supernatant samples were placed in microtitre well plates coated with anti-MMP-9 (100 μl /well). The plates were incubated overnight at 4°C . The following day, *p*-aminophenylmercuric acetate was added to the wells for measuring "total" MMP-9 (pro- and active MMP-9). Buffer alone was added to the wells for measuring "active" (endogenous active MMP-9) MMP-9. Detection agent was then added to all wells (50 μl /well), and the plate was read at 405 nm ($t = 0$ min) and again after a 2-h incubation at 37°C . The value of MMP-9 was standardized by the protein concentration. All measurements were run in duplicate.

ELISA measurement of TIMP-1 and TIMP-2. Commercially available ELISA kits (Daiichi Fine Chemical, Toyama, Japan) were used to measure TIMP-1 and TIMP-2 levels in supernatants according to the manufacturer's instructions (13, 17, 20). Briefly, standards and samples were incubated in microtitre wells coated with anti-TIMP-1 and anti-TIMP-2 antibody. Peroxidase-labeled antibodies directed to the respective TIMPs were added to the corresponding wells. Visualization of the presence of the peroxidase label was achieved using the *o*-phenylenediamine substrate (TIMP-1) or tetramethylbenzidine substrate (TIMP-2). The plates were read at 490 (TIMP-1) or 450 (TIMP-2) nm. Values of TIMPs were standardized by the protein concentration. Since the ELISA systems have some degree of intraplate and interplate variability (<15%) (7), all measurements were run in duplicate to quadruplicate.

Myocardial RNA extraction and reverse transcription. Total RNA was extracted from the risk area (anterior wall) of the LV free wall by an acid guanidium thiocyanate-phenol chloroform method (Isogen, Nippon Gene). First-strand cDNA was synthesized using reverse transcriptase with random hexamer primers from 1 μg of total RNA in a final volume of 20 μl , according to the manufacturer's protocol (ReverTra Ace, Toyobo).

Real-time quantitative reverse transcription-PCR. To analyze TIMP-1 gene expression in myocardial tissue, real-time polymerase chain reaction (PCR) amplification was performed with SYBR Premix Ex Taq (Perfect Real Time; TaKaRa, Japan) using the ABI PRISM 7500 sequence detection system (Applied Biosystems). For standardization and quantification, rabbit glyceraldehyde 3-phosphate dehydrogenase (GAPDH) was amplified simultaneously. The respective PCR primers were designed from GenBank databases (Table 1). The PCR consisted of initial treatments (50°C , 2 min; and 95°C , 10 min) followed by 40 three-step cycles (denaturation 94°C , 10 s; annealing 60°C , 10 s; and extension 72°C , 40 s). Fluorescence was detected at the end of every extension phase (72°C). After PCR amplification, dissociation curves were constructed to confirm the formation of the intended PCR products. Relative expression of TIMP-1 to the GAPDH levels was calculated as described previously (28, 45).

Hemodynamic data analysis. The following hemodynamic parameters were determined from hemodynamic data: HR, mean arterial pressure, maximum first derivative of LVP (LV $\text{dP}/\text{dt}_{\text{max}}$), and fractional shortening of anterior-lateral wall (FS). End diastole and end ejection were defined as the peak of R wave of ECG and the peak of minimum first derivative of LVP, respectively. FS was calculated as

Table 1. Probes used for real-time PCR

Assay	Sequence	Accession Number
TIMP-1		
Forward	5'-CAACTCGGACCTTGTGCATCAG-3'	AY829731
Reverse	5'-CGGTCAAATCCTTTGAACATCT-3'	
GAPDH		
Forward	5'-GGAGAAAGCTGCTAAGTATGACG-3'	L23961
Reverse	5'-CACTGTTGA AGTCGCGAGGAG-3'	

TIMP-1, tissue inhibitor of matrix metalloproteinase-1.

the ratio of systolic stroke change in segmental length and end-diastolic length of the anterior-lateral wall (36).

Cardiac Microdialysis Study

Experimental preparation. Experimental preparation was the same as described above in *I/R Study*, except that no coronary artery occlusion was performed. A microdialysis probe was implanted into the LV anterior wall. Heparin sodium (200 U/kg) was administered intravenously to prevent blood coagulation (19).

Dialysis technique. The materials and properties of the dialysis probe have been described (19). Briefly, we designed a hand-made long transverse dialysis probe. One end of a polyethylene tube (25 cm long, 0.5 mm OD, and 0.2 mm ID) was dilated with a 27-gauge needle (0.4 mm OD). Each end of the dialysis fiber (8 mm long, 0.215 mm OD, 0.175 mm ID, and 300 Å pore size; Evaflex type 5A, Kuraray Medical, Tokyo, Japan) was inserted into the polyethylene tube and glued.

Recovery of TIMP-1 passing through the dialysis fiber membrane was evaluated *in vitro*. The dialysis probe ($n = 4$) was immersed in Ringer solution (in mM; 147.0 NaCl, 4.0 KCl, and 2.25 CaCl₂) containing Tween 20 (0.1%) and various concentrations of TIMP-1 (10–40 ng/ml, free form of human TIMP-1, Daiichi Fine Chemical). The dialysis probe was perfused with Ringer solution at a rate of 2.5 μ l/min using a microinjection pump (model CMA/102, Carnegie Medicine). We measured the concentration of TIMP-1 in the dialysate sample using an ELISA kit. The relative recovery of TIMP-1 was calculated as the ratio of TIMP-1 concentration in dialysate to its concentration in the medium surrounding the probe (11, 22). The relative recovery of TIMP-1 was $11.1 \pm 0.3\%$. Recovery was constant between probes and within the probe for the TIMP-1 concentration range studied.

A fine-guiding needle (25 mm long, 0.51 mm OD, and 0.25 mm ID) was used for implantation of the dialysis probes. The guiding needle was connected to the dialysis probe with a stainless steel rod (5 mm long and 0.25 mm OD). Experimental protocols were initiated 2 h after implanting the dialysis probe. The dialysate sampling period was set at 60 min and was performed taking into account the dead space volume between the dialysis membrane and the sample tube.

Experimental protocol. After baseline dialysate was sampled and baseline hemodynamic data were recorded, the animals were randomized into the following three groups: 1) VNS group ($n = 5$), in which electrical stimulation of vagal nerve was performed while the LV wall was perfused with Ringer solution via the dialysis probe; 2) ACh group ($n = 8$), in which the LV wall was perfused with Ringer solution containing ACh (1 mM); and 3) ACh-atropine (Atr) group ($n = 7$), in which the LV wall was perfused with Ringer solution containing ACh (1 mM) and Atr (0.2 mM). At 150 min after randomization, dialysate sampling and hemodynamic data recording were performed.

At the end of the experiment, the animal was euthanized. From selected hearts, transmural blocks of the LV free wall containing the dialysis probe were fixed in 4% paraformaldehyde for immunohistochemistry.

Immunohistochemistry and confocal microscopy. To investigate the distribution of TIMP-1, we performed confocal image analysis of LV tissue stained with anti-TIMP-1 antibody. Fixed blocks of LV tissues were washed in 0.1 mol/l phosphate buffer (pH 7.4), embedded in paraffin, and sectioned at a thickness of 5 μ m. Sections were deparaffinized using xylene, rehydrated with serial grades of ethanol, and followed by hydration with distilled water. For antigen retrieval of TIMP-1 protein, specimens were immersed in a vessel filled with Target Retrieval Solution (pH 6.1; DAKO). The vessel containing the specimens was autoclaved at 121°C for 20 min. The slides were then allowed to cool at room temperature for 20 min to complete antigen unmasking. The sections were then incubated for 30 h with a mouse anti-TIMP-1 antibody (7-6C1, Daiichi Fine Chemical) diluted 1:5 and

then incubated for 2 h in Alexa-488-conjugated goat anti-mouse Ig-G (Molecular Probes) diluted 1:200. Fluorescence of Alexa-488 was observed with a confocal laser-scanning microscope system (FV 300, Olympus). Reconstructed projection images were obtained from serial optical sections recorded at an interval of 0.5 μ m.

Exclusion Criteria

Animals were excluded from the study when the following criteria were met: 1) in the *I/R* study, coronary artery occlusion did not produce substantial regional dysfunction (FS of the risk area after occlusion was not <20% of the baseline value); 2) intractable ventricular fibrillation or atrial tachycardia occurred; and 3) the animal died during the surgical procedure, and the protocol was not completed.

Statistical Analysis

All data are presented as means \pm SE. Tukey-Welch's step-down multiple comparison test was used to determine the significance of differences among groups. *P* values <0.05 were considered statistically significant.

RESULTS

I/R Study

As shown in Fig. 1A, zymography of the myocardial extracts detected two bands at 92 and 72 kDa, corresponding to MMP-9 and MMP-2, respectively. Densitometric analysis demonstrated that relative MMP-9 level increased to a similar degree in the *I/R* and *I/R-VS* groups compared with the sham and VS groups (Fig. 1B). The relative MMP-2 level decreased in the *I/R* group compared with the sham and *I/R-VS* groups (Fig. 1C).

Bioactivity assays demonstrated that myocardial levels of total MMP-9 protein increased to a similar degree in the *I/R* and *I/R-VS* groups compared with sham and VS groups (Fig. 2A). Levels of endogenous active MMP-9 protein also increased in the *I/R* and *I/R-VS* groups compared with the sham and VS groups (Fig. 2B). The level of active MMP-9 in the *I/R-VS* group was significantly lower than that in the *I/R* group (<50%, $P < 0.01$).

The myocardial level of TIMP-1 protein increased in the VS and *I/R-VS* groups compared with the sham and *I/R* groups (Fig. 3A). There was no significant difference in the myocardial level of TIMP-2 protein among the four groups (Fig. 3B). TIMP-1 mRNA as measured by real-time RT-PCR was increased in the *I/R-VS* group compared with the sham, VS, and *I/R* groups (Fig. 3C).

Table 2 summarizes the data of systemic hemodynamics and LV function during the *I/R* study. In the VS and *I/R-VS* groups, HR decreased significantly compared with sham and *I/R* values at 60 and 240 min. In the *I/R* and *I/R-VS* groups, FS was depressed during ischemia with only partial recovery after reperfusion. In the *I/R* and *I/R-VS* groups, sonomicrometry demonstrated early systolic bulging of the anterior LV wall during ischemia as reflected by negative FS at the 60-min time point. There was no significant difference in LV dp/dt_{max} and FS between the *I/R* and *I/R-VS* groups at 60 and 240 min.

Cardiac Microdialysis Study

Figure 4 presents dialysate TIMP-1 concentrations in response to electrical stimulation of the vagal nerve, to perfusion of ACh, and to perfusion of ACh with Atr. There were no

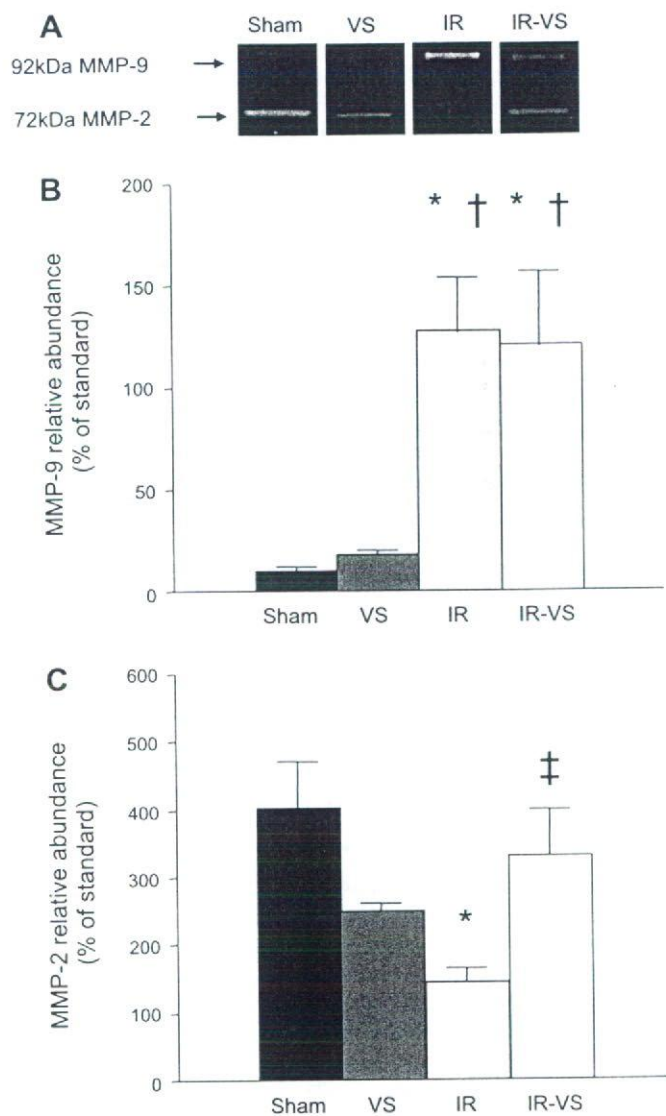


Fig. 1. Zymographic analysis of matrix metalloproteinase (MMP)-9 and -2 proteins in isolated myocardium. Sham, no myocardial ischemia and no vagal stimulation; VS, no myocardial ischemia with vagal stimulation; I/R, myocardial ischemia-reperfusion; I/R-VS, myocardial ischemia-reperfusion with VS. A: representative zymogram showing MMP-9 at 92 kDa and MMP-2 at 72 kDa. B: densitometric analysis of relative MMP-9 content expressed as percentage of standard. C: densitometric analysis of relative MMP-2 content expressed as percentage of standard. Data are means \pm SE. * $P < 0.01$ vs. sham; † $P < 0.01$ vs. VS; ‡ $P < 0.05$ vs. I/R.

significant differences in baseline TIMP-1 concentrations among the three groups. At 150 min, dialysate TIMP-1 concentration was significantly higher in the VNS and ACh groups than in the ACh-Atr group ($P < 0.05$).

Figure 5 depicts representative microscopic findings of LV tissue around the microdialysis probes in the VNS, ACh, and ACh-Atr groups. Hematoxylin-eosin-stained sections demonstrated only a minimum hemorrhage around the dialysis probe (Fig. 5, A–C). TIMP-1-positive cardiomyocytes were detected sparsely but in diffuse distribution throughout the myocardium in the VNS group (Fig. 5D). TIMP-1-positive cardiomyocytes were detected over a relatively wide area around the dialysis probe in the ACh group (Fig. 5E). TIMP-1-positive cardiomyocytes were also detected but localized close to the dialysis

probe in the ACh-Atr group (Fig. 5F). Immunoreactive signals of TIMP-1 were restricted to the cytoplasm of cardiomyocytes in all the groups (Fig. 5, G–I).

Table 3 summarizes the data of systemic hemodynamics and LV function during the cardiac microdialysis study. In the VNS group, HR decreased significantly compared with that in the ACh and ACh-Atr groups at 150 min. In the ACh and ACh-Atr groups, topical perfusion of ACh or ACh with Atr did not affect the systemic hemodynamics and the LV functions. Except for HR, there were no significant differences in other hemodynamic parameters among the three groups.

DISCUSSION

The major new findings of the present study were as follows. In ischemia-reperfused myocardium, stimulation of the efferent vagal nerve increased TIMP-1 mRNA and protein levels and reduced endogenous active MMP-9 protein. In normal myocardium, VNS or topical perfusion of ACh through a microdialysis probe increased dialysate TIMP-1 protein level. An increase in the dialysate TIMP-1 protein level induced by ACh perfusion was suppressed by coproduction of Atr.

The robust increase in total MMP-9 levels after reperfusion in this study (Figs. 1B and 2A) might be mainly due to the

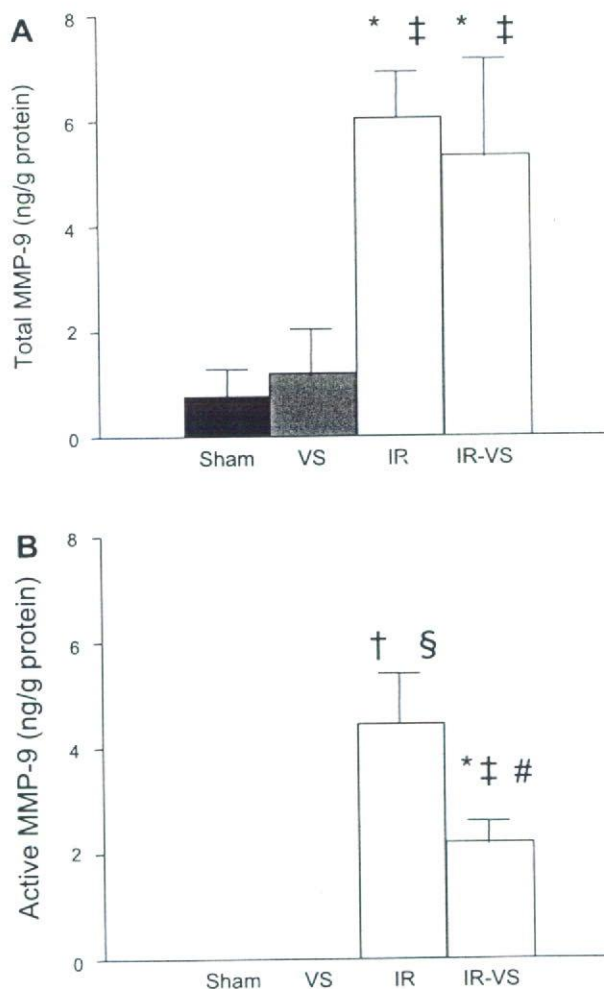


Fig. 2. Bioactivity assay of total (A) and active (B) MMP-9 protein. * $P < 0.05$; † $P < 0.01$ vs. sham; ‡ $P < 0.05$; § $P < 0.01$ vs. VS. # $P < 0.01$ vs. I/R.

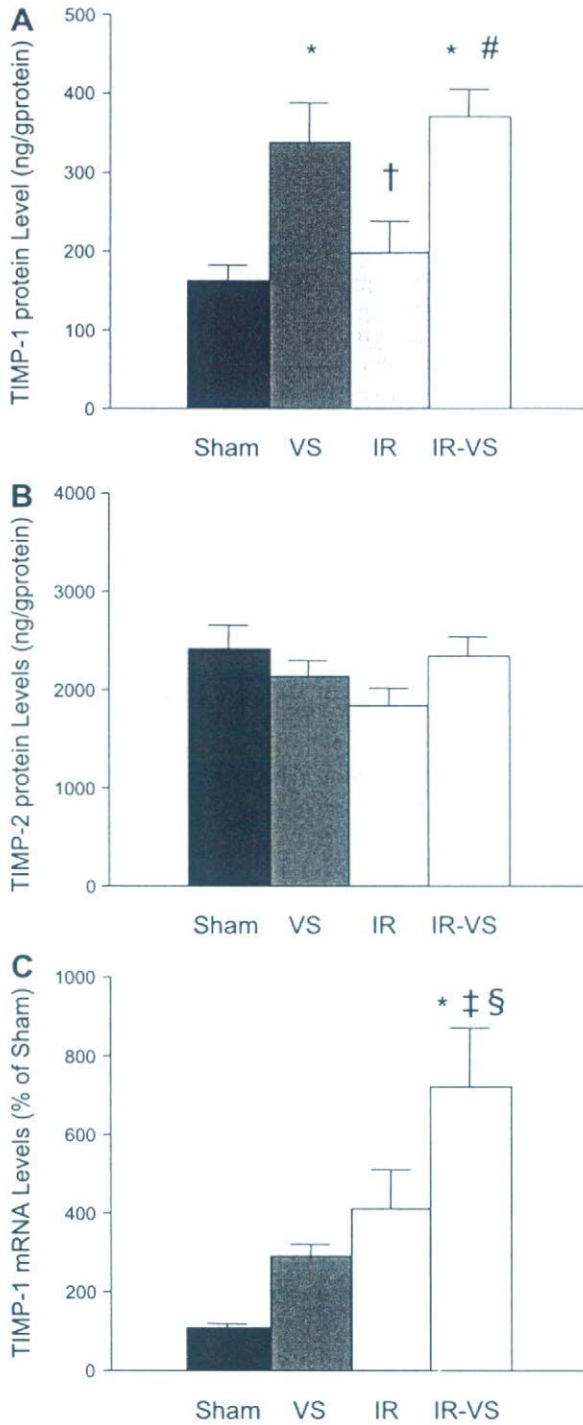


Fig. 3. ELISA measurement of tissue inhibitor of MMP (TIMP)-1 (A) and -2 (B) protein. Real-time RT-PCR analysis of TIMP-1 mRNA expressed as percentage of sham (C). **P* < 0.01 vs. sham; †*P* < 0.05; ‡*P* < 0.01 vs. VS; §*P* < 0.05; #*P* < 0.01 vs. I/R.

infiltrated neutrophils. Although all cell types, including cardiomyocytes (25, 34) and endothelial cells (41), express MMP-9, neutrophil is an important source of MMP-9 after I/R (26). The level of endogenous active MMP-9 was lower in the I/R-VS group than in the I/R group (Fig. 2B). Increased expression of TIMP-1 by VNS (Fig. 3) likely inhibited the conversion of pro-MMP-9 to active MMP-9 and/or inhibited

Table 2. Hemodynamic parameters during I/R study

	Baseline	60 min	240 min
HR, beats/min			
Sham	317 ± 9	334 ± 7	326 ± 9
VS	281 ± 14	215 ± 17*‡	238 ± 19*‡
I/R	306 ± 9	316 ± 9	314 ± 8
I/R-VS	301 ± 7	217 ± 5*‡	228 ± 8*‡
MAP, mmHg			
Sham	92 ± 3	93 ± 4	92 ± 3
VS	98 ± 4	91 ± 5	89 ± 5
I/R	102 ± 3	95 ± 4	88 ± 6
I/R-VS	99 ± 4	88 ± 4	83 ± 2
LV dP/dt _{max} , mmHg/s			
Sham	5,119 ± 263	5,308 ± 388	4,819 ± 339
VS	5,040 ± 381	3,993 ± 319	4,140 ± 302
I/R	5,524 ± 423	5,276 ± 404	4,514 ± 467
I/R-VS	5,672 ± 360	4,549 ± 250	4,079 ± 188
FS, %			
Sham	10.8 ± 0.9	10.1 ± 1.0	9.3 ± 1.0
VS	12.2 ± 1.1	11.1 ± 1.2	10.4 ± 1.6
I/R	8.7 ± 0.8	-0.6 ± 0.6*†	0.1 ± 0.8*†
I/R-VS	8.5 ± 1.3	-0.6 ± 0.4*†	1.5 ± 0.7*†

Values are means ± SE. Sham group, no myocardial ischemia and no vagal stimulation (VS); VS group, no myocardial ischemia with VS; I/R group, myocardial ischemia-reperfusion (I/R); IR-VS, myocardial I/R with VS; HR, heart rate; MAP, mean arterial pressure; LV dP/dt_{max}, maximum first derivative of left ventricular (LV) pressure; FS, fractional shortening of anterior wall (risk area). **P* < 0.01 vs. sham; †*P* < 0.01 vs. VS; ‡*P* < 0.01 vs. I/R.

active MMP-9 itself more potently than in the case without VNS (14). Oxygen free radical induces expression and activation of MMP-9 (17, 41). Reduction of HR by VNS probably reduced myocardial oxygen consumption, ameliorated myocardial ischemia, and reduced oxygen free radicals (30). This may contribute to some extent to the reduction of active MMP-9 in the I/R-VS group.

In the I/R study, TIMP-1 mRNA was significantly higher in the I/R-VS group compared with the sham, VS, and I/R groups (Fig. 3C). TIMP-1 mRNA appeared higher in the VS and I/R groups compared with the sham group, although the differences were not significant. Stapel et al. (38) noted increased expression of TIMP-1 mRNA after myocardial I/R in mice. Proinflammatory cytokines such as interleukin-1β induced by

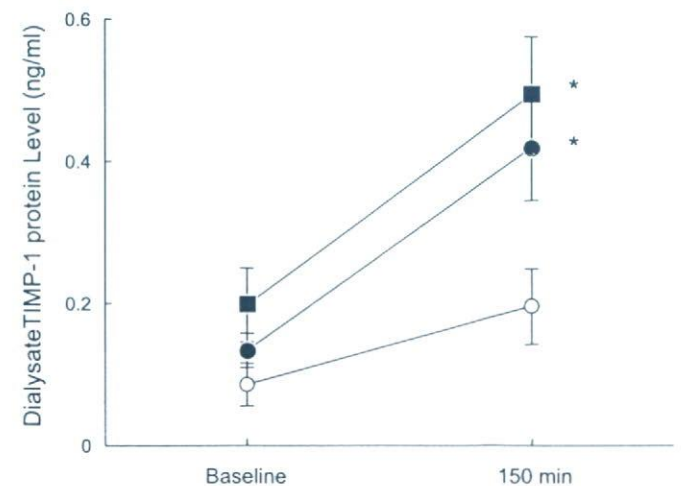


Fig. 4. Dialysate TIMP-1 protein concentration in response to vagal nerve stimulation (■), perfusion of acetylcholine (ACh; ●), or ACh with atropine (Atr) (○). **P* < 0.05 vs. perfusion of ACh with Atr.

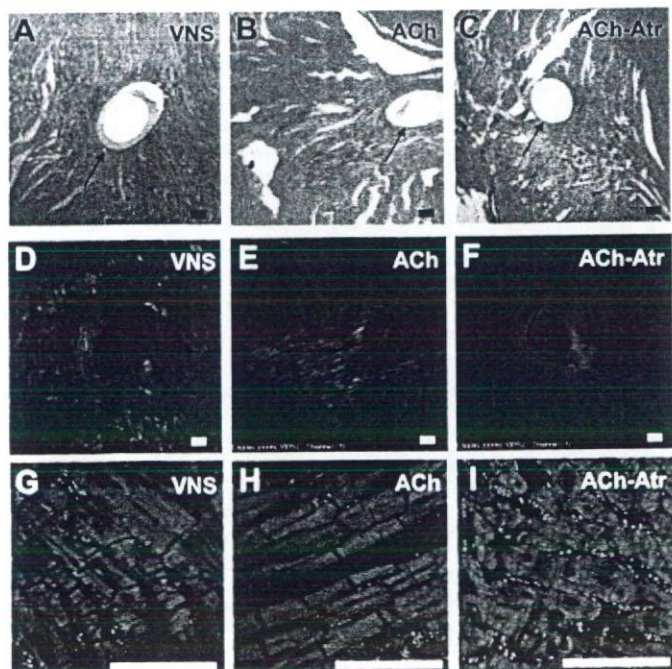


Fig. 5. Representative microscopic finding of left ventricular (LV) tissue implanted with microdialysis probe. A–C: hematoxylin and eosin-stained section of LV tissue perfused with Ringer solution under vagal nerve stimulation (VNS; A), perfused with ACh (B), and perfused with ACh and Atr (ACh-Atr; C). D–F: anti-TIMP-1 antibody (green)-immunostained sections of LV tissue perfused with Ringer solution under VNS (D), perfused with ACh (E), and perfused with ACh-Atr (F). G–I: higher magnifications of D–F, respectively. Arrows indicate dialysis probes. Bar = 100 μ m.

myocardial ischemia are known to induce TIMP-1 (4). VNS and myocardial ischemia likely exerted an additive effect on the induction of TIMP-1 mRNA in the I/R-VS group. TIMP-1 protein levels in the VS and I/R-VS groups were significantly elevated compared with the sham and I/R groups (Fig. 3A). Figure 3, A and C, indicates dissociation between TIMP-1 mRNA and protein synthesis among the four groups. If the TIMP-1 protein level had correlated with the mRNA level, TIMP-1 protein level in the I/R and I/R-VS groups should have been higher than those presented in Fig. 3A. In myocardial ischemia, protein synthesis decreases owing to the inhibition of peptide chain elongation (8, 18). This may have partially inhibited TIMP-1 protein synthesis in the I/R and I/R-VS groups.

In the cardiac microdialysis study, the ACh-induced release of TIMP-1 was mediated by muscarinic ACh receptors because Atr blocked the increase in TIMP-1 in response to ACh stimulation (Fig. 4). TIMP-1 was produced by cardiomyocytes (Fig. 5, G–I). These findings suggest that VNS may induce TIMP-1 mRNA expression through muscarinic ACh receptors in cardiomyocytes and increase TIMP-1 protein content in myocardium. The distribution of TIMP-1-positive cardiomyocytes was different among the three groups (Fig. 5, D–F). This may reflect differences in the distribution of ACh among the three groups. ACh probably had a diffuse distribution in the myocardium in the VNS group but was concentrated around the dialysis probe in ACh group, whereas the effect of ACh concentrated around the dialysis probe was antagonized by Atr in the ACh-Atr group.

In addition to cardiomyocytes (25, 34), a variety of cell types, such as fibroblasts (14) and endothelial cells (6), produces and secretes TIMP-1. TIMP-1 expression in these cell types is low in the basal condition but is transcriptionally induced by various agents, including the cytokines, serum, growth factors, and phorbol esters (14). The signal transduction pathway from muscarinic ACh receptor stimulation to the induction of the TIMP-1 gene is not clear. Further elucidation of this is not in the scope of this study. ACh increases the production of nitric oxide from cardiomyocytes (9). Nitric oxide induces TIMP-1 gene expression by activating the transforming growth factor- β /Smad signaling pathway in glomerular mesangial cells in the kidney (2). These mechanisms may be involved in the increases in TIMP-1 mRNA and protein induced by VNS in myocardial I/R observed in the present study. Further studies are clearly required to elucidate these issues.

Myocardial expression of TIMP-2 was not modified by VNS (Fig. 3B). Contrary to the highly responsive nature of TIMP-1 expression to stimuli, TIMP-2 expression is, for the most part, constitutive (14). Previous studies demonstrated that ischemic injury or change in loading condition had little effect on myocardial expression of TIMP-2 (24, 25, 29). Myocardial content of MMP-2 decreased after I/R, and the decrease was inhibited by VNS (Fig. 1C). Cheung et al. (5) demonstrated that MMP-2 was released from the myocardium into the coronary effluent following myocardial I/R, resulting in the depletion of myocardial content of MMP-2.

In the present study, VNS did not prevent contractile dysfunction after I/R (Table 2). Actions of MMP and TIMP did not seem to be responsible for acute mechanical changes. Lu et al. (29) demonstrated that treatment with the MMP inhibitor failed to prevent acute myocardial dysfunction and regional expansion after I/R injury. The duration of reperfusion in our study (180 min) and that in Lu et al. (90 min) (29) may be too short to detect a significant influence of MMP and TIMP on regional LV function, which may become evident after a longer period of reperfusion.

Table 3. Hemodynamic parameters during cardiac microdialysis study

	Baseline	150 min
HR, beat/min		
VNS	286 \pm 7	227 \pm 7*†
ACh	303 \pm 16	308 \pm 9
ACh-Atr	304 \pm 14	298 \pm 16
MAP, mmHg		
VNS	101 \pm 8	103 \pm 8
ACh	93 \pm 3	100 \pm 4
ACh-Atr	87 \pm 3	92 \pm 6
LV dP/dt _{max} , mmHg/s		
VNS	5,050 \pm 588	4,768 \pm 475
ACh	5,203 \pm 345	5,488 \pm 400
ACh-Atr	4,519 \pm 269	4,718 \pm 450
FS, %		
VNS	7.4 \pm 1.8	7.2 \pm 1.9
ACh	5.0 \pm 1.2	4.9 \pm 1.2
ACh-Atr	5.4 \pm 0.5	5.0 \pm 0.5

Values are means \pm SE. VNS group, LV tissue was perfused with Ringer solution via a dialysis probe under vagal nerve stimulation; ACh group, LV tissue was perfused with Ringer solution containing ACh (1 mM) via a dialysis probe; ACh-Atr group, LV tissue was perfused with ACh (1 mM) and atropine (0.2 mM) via a dialysis probe. * P < 0.01 vs. ACh; † P < 0.01 vs. ACh-Atr.